nature nanotechnology

SUPPLEMENTARY INFORMATION

DOI: 10.1038/NNANO.2014.282

Mass spectrometry imaging reveals the sub-organ distribution of carbon nanomaterials

*Suming Chen, Caiqiao Xiong, Huihui Liu, Qiongqiong Wan, Jian Hou, Qing He, Abraham Badu-Tawiah, and Zongxiu Nie**

Table of Contents

Materials and methods

High purified carboxylic multi-walled carbon nanotubes (CNTs, purity: > 98%, -COOH content: ~ 10%, OD: 10-20 nm, ID: 5-10 nm, length: 0.5-2 μm) made by chemical vapor deposition method and single layer graphene oxide (GO, purity: > 99%, diameter: 1-5 μm, thickness: 0.8-1.2 nm, single layer ratio: ~ 99%) were purchased from Nanjing XFNANO Materials Tech Co., Ltd (Nanjing, China) and characterized carefully by high-resolution transmission electron microscopy (HRTEM, JEM-2011, JEOL, Japan), X-ray photoelectron spectroscopy (XPS, ESCALab 250Xi, Thermo Scientific, USA) and atomic force microscopy (AFM, Nano IIIa, Veeco Company, USA). The sizes statistics of CNTs and carbon nanodots (diameter, length, OD and ID) were measured by Adobe Photoshop software (version 7.0). XPS was performed using 200 W monochromated A1 Kα radiation. The 500 μm X-ray spot was used for XPS analysis. The base pressure in the analysis chamber was about 3×10^{-10} mbar. Typically the hydrocarbon C1s line at 284.8 eV from adventitious carbon is used for energy referencing. The XPS peak fitting programme XPSPEAK 4.1 (written by Raymund Kwok) was used for the spectra processing.

Oxidized CNTs was prepared from high purified carboxylic multi-walled carbon nanotubes. The purchased CNTs (100 mg) was mixed with HNO_3 (5 M, 20 mL) and refluxed for 12 hours. After cooling to room temperature, the mixture was first neutralized by Na_2CO_3, and then dialyzed against de-ionized water through a dialysis membrane (MWCO 3500) for 48 h. The lyophilized oxidized CNTs was used to prepare the solutions on-demand by weighting method. The material was characterized by X-ray photoelectron spectroscopy to evaluate the oxidation component.

The carbon nanodots (CDs) was prepared by refluxing candle soot method according to our previous report with slight modification.[1] Candle soot was collected by putting a glass plate on the top of burning unscented candles. Then candle soot (100 mg) was mixed with HNO_3 (5 M, 20 mL) and refluxed for 12 hours. After

cooling to room temperature, the mixture was first neutralized by Na_2CO_3, and then the supernatant was collected by centrifugation (14000 g for 30 min). Subsequently, excess sodium borohydride (0.5 g) was added to the obtained CDs solution and was stirred gently overnight at room temperature. Finally, the CDs solution was obtained by dialyzing against de-ionized water through a dialysis membrane (MWCO 3500) for 48 h. The lyophilized CDs was used to prepare the solutions on-demand by weighting method.

Unless otherwise stated, the chemicals were used without further purification. Solvents were purchased and were at least analytical grade. The de-ionized water was obtained from a Milli-Q system (Millipore, MA, USA) and was used throughout.

Preparation of the tissue samples for TEM study

The preparation steps of sample for TEM observation is listed as follows: (1) the organs (e.g. lung, liver, spleen) of CNMs-injected mice were harvested after 24 h post-injection. The interested tissues were cut into blocks of about 1 mm^3, and then put into the 2% glutaraldehyde solutions in PBS (pH 7.4) for fixation about 4 h. (2) The fixed samples were dehydrated with serials of ethanol solutions (30%, 50%, 70%, 80%, 90%, 95%, 100%), each for 7 min. Then the dehydrated samples were immersed into anhydrous acetone for three times, each for 15 min. After immersed in the solution of acetone and embedding agent (epoxy resin, dodecylsuccinic, anhydride dibutylphthalate and ethylenediamine mixture) (1 : 2, v/v) at 35 °C for 2 h, the samples were immersed in pure embedding agent at 35 °C overnight. Finally, the samples were polymerized in embedding agent at 60 °C for 48 h. (3) The embedded tissue samples were sectioned with an ultramicrotome at about 70 nm for TEM imaging. The TEM sections were cut onto micro-grids.

Quantification of CNMs in organs

To exactly quantify the CNMs in different mice organs, the imaging mass spectrometry method combined with homogenate strategy was developed. In brief, the

slices of tissue homogenate spiked with different concentrations of individual material (CNTs, GO and CDs) were subjected to LDI IMS analysis to obtain the calibration curves. Note that in order to obtain the reliable quantitative results, different tissue homogenate (e.g. heart, liver, spleen, lung, kidney and brain) spiked with serials of CNMs were used to plotted the each calibration curve, respectively. Then the CNMs-injected mice' tissue homogenate slices were analyzed with the same protocol. The amount of individual material in various organs can be calculated according to the calibration equations based on the average intensity of C_6^- (*m/z* 72.0). Three mice were used per group at each time point to obtain the average value and standard deviation for biodistribution measurements.

The detailed procedures were described as follows (Supplementary Fig. 18): (1) Preparation of the homogenate. The harvested and weighed normal organ was cut into small pieces and transferred into the centrifuge tube. Then 1% sodium dodecyl sulfate (SDS) solution was added (6 μLmg^{-1} tissue) for lysis using a homogenizer. After heating at 70 °C for 2 hours, clear homogenate tissue solutions were obtained and spiked with different concentration of CNMs. The CNMs-injected mice' tissue homogenate was prepared by the same procedures. (2) Preparation of the homogenate slices. Cut the end from a 1 mL disposable syringe (ID = 0.5 cm). Withdraw the plunger to suck a volume of around 0.1 mL homogenate at the open end of the syringe. Subsequently, freeze the homogenate in the syringe by placing it into liquid nitrogen for several seconds. The cylindroid solid homogenate was pushed out and sectioned at −20 °C into round slice of 30 μm thickness in a cryostat. The slices were immediately thaw-mounted on ITO-coated microscopic glass slides and then dried under vacuum for 30 min before mass spectrometry measurement. (3) Mass spectrometry measurement. The glass slide with homogenate slices was mounted on the holder and entered into the MALDI mass spectrometer for imaging analysis. The rectangular region was selected on each slice and measured with 100 μm laser resolution. (4) Calculate the amounts of CNMs in organ. The average ion intensity of C_6^- (*m/z* 72.0) was chose to represent the amount of CNMs. After plot the calibration curve (average intensity *vs* concentration), the concentration of the CNMs-injected tissue homogenate

can be calculated. The calibration curves of heart, kidney, spleen, lung and kidney were plotted individually using normal homogenates spiked with CNTs, GO and CDs, respectively. The percent injected dose (%ID), percent injected dose per gramme of tissue (%ID/g) and concentration (μg/g) for each carbon nanomaterial were calculated by the following equations:

$$\%\ \mathrm{ID} = \frac{[\mathrm{CNMs}]_{\mathrm{lysate}} \times \mathrm{V}_{\mathrm{lysate}}}{[\mathrm{CNMs}]_{\mathrm{injected}} \times \mathrm{V}_{\mathrm{injected\ CNMs}}} \times 100\%$$

$$\%\ \mathrm{ID/g} = \frac{[\mathrm{CNMs}]_{\mathrm{lysate}} \times \mathrm{V}_{\mathrm{lysate}}}{[\mathrm{CNMs}]_{\mathrm{injected}} \times \mathrm{V}_{\mathrm{injected\ CNMs}} \times \mathrm{tissue\ weight}} \times 100\%$$

$$\mu\mathrm{g/g} = \frac{[\mathrm{CNMs}]_{\mathrm{lysate}} \times \mathrm{V}_{\mathrm{lysate}}}{\mathrm{tissue\ weight}}$$

Quantification of CNTs in different regions of spleen

The characteristic distribution of CNTs in spleen inspires us to quantify them separately for different regions, such as red pulp, white pulp and marginal zones. However, the absolute quantification of analyte in tissue using direct mass spectrometry imaging methods is still a great challenge. Koeniger et al.[2] demonstrated that, without internal standard, the intensity of an analyte detected by MALDI imaging could be correlated to its quantity measured in a pool of serial sections. From this correlation, a conversion factor of fg/ion count was used to quantitate MSI responses at the pixel level. This method can provide good results for the quantification of small molecules in tissues and the amount of analyte is readable from the image.[3] Here we attempted to employ this approach for quantifying CNTs in spleen as the following steps.

Nine of Male 6- to 8-week-old Kunming mice were divided into three groups (three for each group). 100 μL of different concentration of CNTs (0.25, 0.5 and 1 $\mathrm{mgmL^{-1}}$) was administered intravenously. The mice were sacrificed and dissected 24 h after the intravenous administration. Spleen was harvested and flash-frozen by slow immersion in liquid nitrogen to avoid shattering and then stored in fridge at −20 °C. The sections

are collected in the following order: (1) ten 10 μm tissue sections were collected into a pre-weight 1 mL plastic Eppendorf tube; (2) three adjacent sections (10 μm) for MSI were each carefully thaw-mounted on ITO-coated microscopic glass slide (Bruker Daltonics) to obain the same area to access section-to-section reproducibility; and (3) ten 10 μm sections were collected and combined with the first 10 sections into the tube. These tissue sections were then subjected to homogenate, section and quantification by the previous described steps. Note that these adjacent 23 of sections were approximately considered to have the same mass, area and contain the same concentration of CNTs. The mass of one section could be obtained by the total mass dividing the amount of the sections. Thus the amount of CNTs in one tissue section can be calculated.

For the MSI of the different tissue sections, negative ion mode was adopted with a spatial resolution of 50 μm after a pixel-shift of 50 μm in both x and y dimensions. The total ion count of each imaging section can be obtained by multiplying average ion intensity by total points in Fleximaging software (Bruker, version 4.0). The ion intensity value of each point was recognized as the ion count. Further, the tissue weight of each pixel area can be calculated by dividing the weight of the section by total pixel point.

In order to quantitate the integrated LDI MSI response and the amounts of analyte per tissue section, the amount of CNTs measured by homogenate quantification is plotted on the ordinate (ng/tissue section) and the MSI response is plotted on the abscissa (ion counts/tissue section) such that the slope of the plot yields an amount of material per MSI count or pg/ion count. For the spleen studied here, a linear and reproducible response can be obtained. The RSD of MSI response for the adjacent sections is ~ 10%, which may benefit from the matrix-free measurement. The slope yielded a conversion factor of 1.8 ± 0.16 fg/ion count. If we do not take into consideration the signal variations due to the ion suppression effects across the tissue section, the quantitative information can be approximately obtain from the MSI image of spleen tissue section. The linear color scale can be converted from MSI ion counts into pg/pixel through the relationship, and the amount of CNTs in the different regions

of spleen tissue section could be easily read based on the color. Further along, the concentrations of CNTs in spleen white pulp, red pulp and marginal zones were quantified. The concentration per pixel was calculated by the equation: concentration (μg/g) = average ion count per pixel × conversion factor (μg/ion count) / tissue weight per pixel (g). Ten of region of interest (ROI) in the LDI MSI image were selected for white pulp, red pulp and marginal zone, respectively. The average ion intensity of ROI can be read from the average mass spectrum by using the FlexImaging software (Bruker, version 4.0). Each ROI contains about 50 pixel points.

Blood assay

Complete blood counts (CBC) and serum biochemical analysis were conducted to further examine the toxicity of CNMs. Typically, 200 μL of 0.5 $mgmL^{-1}$ CNTs and CDs and 200 μL of 0.25 $mgmL^{-1}$ GO were injected into the separate groups (5 mice per group) of mice via the tail vein at different time point (1d, 3d and 7d), respectively. As a control, five mice were injected with 200 μL of physiological saline. For each mouse, about 1.5 mL whole blood was collected from eye socket through a heparin-coated glass capillary. 1 mL of the blood was used for CBC and 0.5 mL for serum biochemical analysis. All the blood assays were performed at the Deyi Diagnostics Corporation (Beijing, China). The analyzed items for CBC are white blood cells, neutrophil, lymphocyte, red blood cells, mean red cells volume, hematocrit, red blood cell distribution width, hemoglobin, mean corpuscular hemoglobin, mean corpuscular hemoglobin concentration, platelet, mean platelet volume, plateletcrit and platelet distribution width. The parameters of the serum biochemical analysis includes: creatinine, total protein, albumin, globulin, alanine aminotransferase (ALT), alkaline phosphatase (ALP), aspartate aminotransferase (AST) and blood urea nitrogen (BUN).

The clearance of CDs over time

To glean the long term fate of CDs, injected mice were sacrificed at 24 h, 60 h, 12 d, 17 d and 30 d p.i. for biodistribution measurements and LDI IMS with three animals per group at each time point. The presence of CDs in all of the organs after 24 h p.i. can be detected. The high level of CDs in liver, spleen and kidney was found. An obvious trend of decreasing amount in all organs was observed from the biodistribution data (Supplementary Fig. 23a), which implied the clearance of CDs from the mice body. Although the decreasing tendency is similar among different kinds of CDs, the clearance rates are not at the same level. Chen reported that the injected diamine-terminated PEG functionalized CDs could be rapidly cleared from more than 10% ID/g in kidney to less than 1% in any of the organ within 24 h.[4] While we found there is still 1.6% ID/g CDs in mouse liver even after 17 d clearance, and CDs can be detected in all the organs even after 30 d clearance except brain. The CDs prepared from carbon nanotubes reported by Liu has the similar long-term retention behavior, more than 2% ID/g was found in mice liver and spleen at 7 d p.i.[5] These differences may be ascribed from the different functionalized surfaces of carbon nanodots derived from varied sources. The LDI IMS images of CDs in kidney tissue over time were in accordance with the quantitative data (Supplementary Fig. 23b). Predominant CDs retained in medulla part of kidney, and the gradually disappeared signal clearly reflected the clearance process of CDs in kidney. The combination of the IMS and quantitative methods provides a more comprehensive and convenient tool for the deep investigation of biodistribution of CNMs in animals.

Tumour cell lines and culture

The S180 sarcoma cell line was tested negative for all relevant murine viruses and mycoplasma using a MAP full-panel test (Taconic, Germantown, NY, USA) prior to use. S180 cell lines were maintained in cell culture until in vivo transplantation. The cells were cultured in DMEM with GlutaMAX-I and HEPES (Invitrogen, Taastrup, Denmark). Penicillin and streptomycin were added to a final concentration of 100

IE/ml and 100 μg/ml, respectively, and fetal calf serum (FCS) was added to a final concentration of 10%. The medium was changed every second day, and the cells were seeded at a density of 4 ~ 5 × 10^5 viable cells/ml. The cells were split when reaching a density of 1 ~ 2 × 10^6 viable cells/ml.

In vivo cell maintenance and induction of subcutaneous tumors

Initially, ascites was induced in Kunming mice by the i.p. injection of 2 × 10^5 S180 cells from an in vitro culture. After approximately two weeks, the mice developed ascites and were euthanized by cervical dislocation. The ascitic fluid was immediately removed by aspiration with a 10 ml syringe with a 19 G needle. The cells were then diluted with physiological saline and were counted. The cells were adjusted to 5 × 10^5 cells/ml in saline, kept at room temperature and used for injection within one hour. The tube containing the cells was inverted several times to maintain the cells in suspension. For the induction of subcutaneous tumours, C57 mice (3 weeks) were acclimatized for about one week and then 100 μL of the treated cells was subcutaneously injected into the right arm armpit. The mice were returned to their cage immediately after injection. After growing for about one week, the tumour could be observed from armpit.

Loading of doxorubicin onto CNTs

Doxorubicin (DOX) loading on to multi-walled carbon nanotubes (CNTs) was done according to the previous report[6] by simply mixing 1 mM DOX with the CNTs at a nanotube concentration of 0.05 mg/mL at various pH = 8 overnight. Unbound excess DOX was removed by filtration through a 10 kDa filter and washed thoroughly with water (over 10 times) and PBS until the filtrate became free of reddish color (corresponding to free DOX). The formed complexes (denoted as CNT-DOX) were then resuspended and stored at 4 °C. UV–Vis absorption spectra of the CNT-DOX complexes were measured by using a TU-1900 spectrophotometer (Purkinje General, Beijing, China). The concentrations of CNTs were determined by the absorbance at

800 nm. The concentration of DOX loaded onto CNTs was measured by the absorbance peak at 490 nm (characteristic of DOX, after subtracting the absorbance of CNTs at that wavelength) with a molar extinction coefficient of 1.05×10^5 $M^{-1}cm^{-1}$. Note that thorough removal of free DOX was carried out by filtration prior to the measurement to accurately assess the amount of DOX loaded onto CNTs.

Intravenous administration of drug-loaded CNTs in tumour-induced mice

After the tumour was grown, the drug-loaded CNTs (CNT-DOX, 1 $mgmL^{-1}$, 100 μL) were administered intravenously to each mouse. After 24 h, the mice were sacrificed by cervical dislocation. Then, the tumours were harvested and further analyzed. Three 10 μm thickness of sections from the middle part of the tumour were used for the LDI-MS imaging, and the rest was converted into homogenate and sectioned for LDI MS quantification. The calibration curve of CNTs in tumour was made by using tumour harvested from mice without injection of CNT-DOX.

Preparation of monolayer molybdenum disulphide (MoS_2)

Lithium intercalation was achieved by immersing 3 g of natural MoS_2 crystals (powder, < 2 μm, 99%, Sigma-Aldrich) in 21 mL of 1.6 M butyllithium solution in hexane (Sigma-Aldrich) for 2 days in a flask filled with argon gas. The Li_xMoS_2 was retrieved by filtration and washed with hexane (60 mL) to remove excess lithium and organic residues. Exfoliation was achieved immediately after this (within 30 min to avoid deintercalation) by ultrasonicating Li_xMoS_2 in water for 1 h. The mixture was centrifuged several times to remove excess lithium in the form of LiOH and unexfoliated material. Finally, the MoS_2 solution was obtained by dialyzing against de-ionized water through a dialysis membrane (MWCO 3500) for 48 h. The lyophilized MoS_2 was used to prepare the solutions on-demand by weighting method. For the MS imaging of the MoS_2 in mouse lung, 100 μL of 1 $mgmL^{-1}$ MoS_2 solution in physiological saline was administered intravenously. The mice were sacrificed and dissected 24 h after the intravenous administration. Lung was harvested and weighed for biodistribution and imaging.

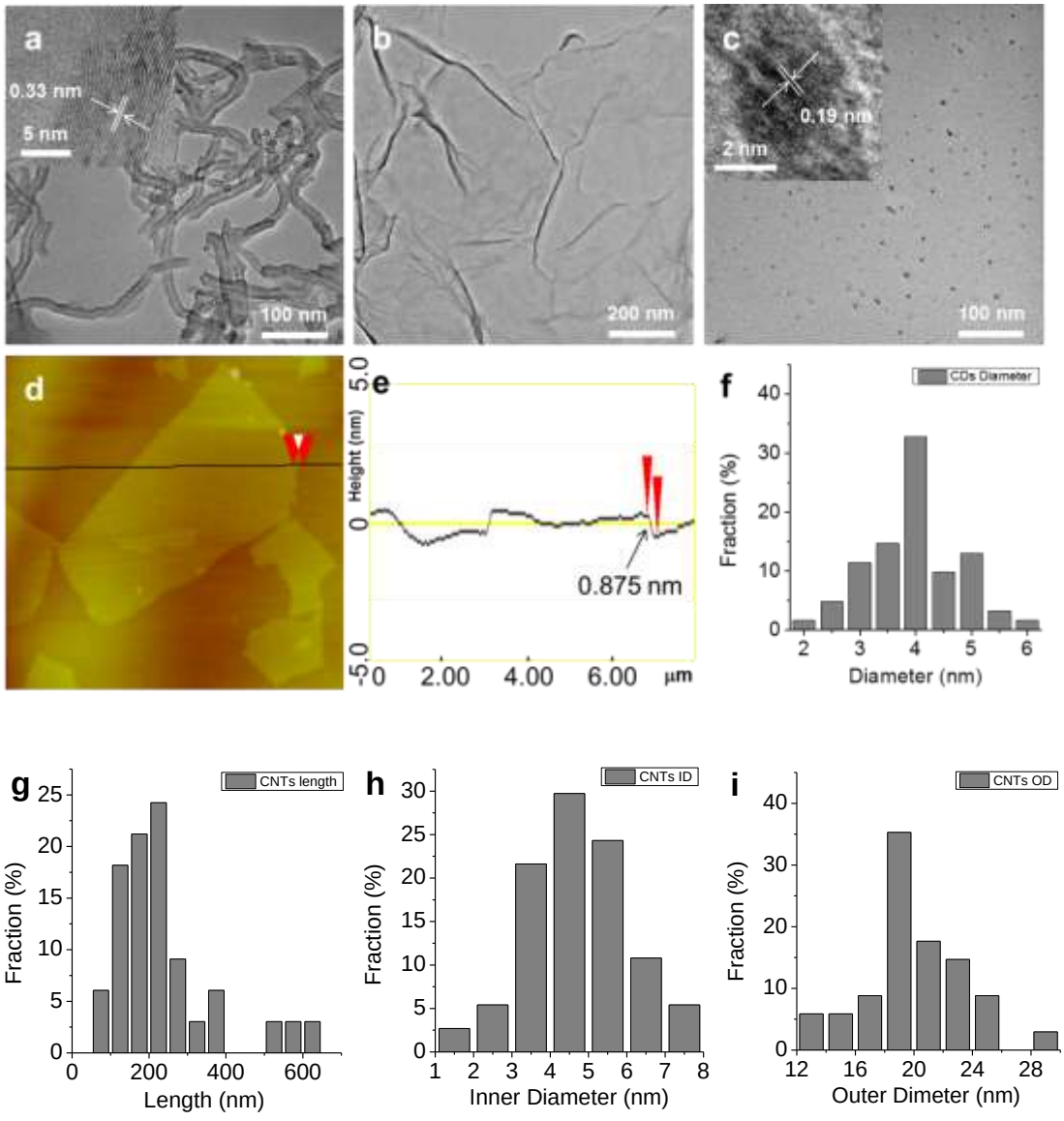

Supplementary Fig. 1. Characterization data of CNTs, GO and CDs. (a) TEM images of CNTs. Inset shows the high-resolution TEM image of carbon nanotube wall. (b) TEM image of GO. (c) TEM images of CDs. Inset shows the high-resolution TEM image of a single carbon dots. (d) AFM image of GO and (e) the corresponding height profile. (f) Particle size distribution histogramme of CDs calculated according to the TEM image. (g) Length distribution histogramme of CNTs. (h) Inner diameter distribution histogramme of CNTs. (i) Outer diameter distribution histogram of CNTs. HRTEM measurements revealed lattice spacing of 0.33 nm and 0.19 nm for CNTs and CDs, which is consistent with the (006) and (104) diffraction planes of sp^2 graphite carbon (insets of a and c). The AFM images indicated the single layer

structure of graphene oxide and the size could up to about 5 μm. The thickness of 0.875 nm in E indicated the single layer structure of graphene oxide. The average diameter of CDs was 3.9 nm with a standard deviation of 0.8 nm. The average length of CNTs was 264 nm with a standard deviation of 146 nm. The average inner diameter of CNTs was 4.7 nm with a standard deviation of 1.1 nm. The average outer diameter of CNTs was 19.2 nm with a standard deviation of 3.4 nm.

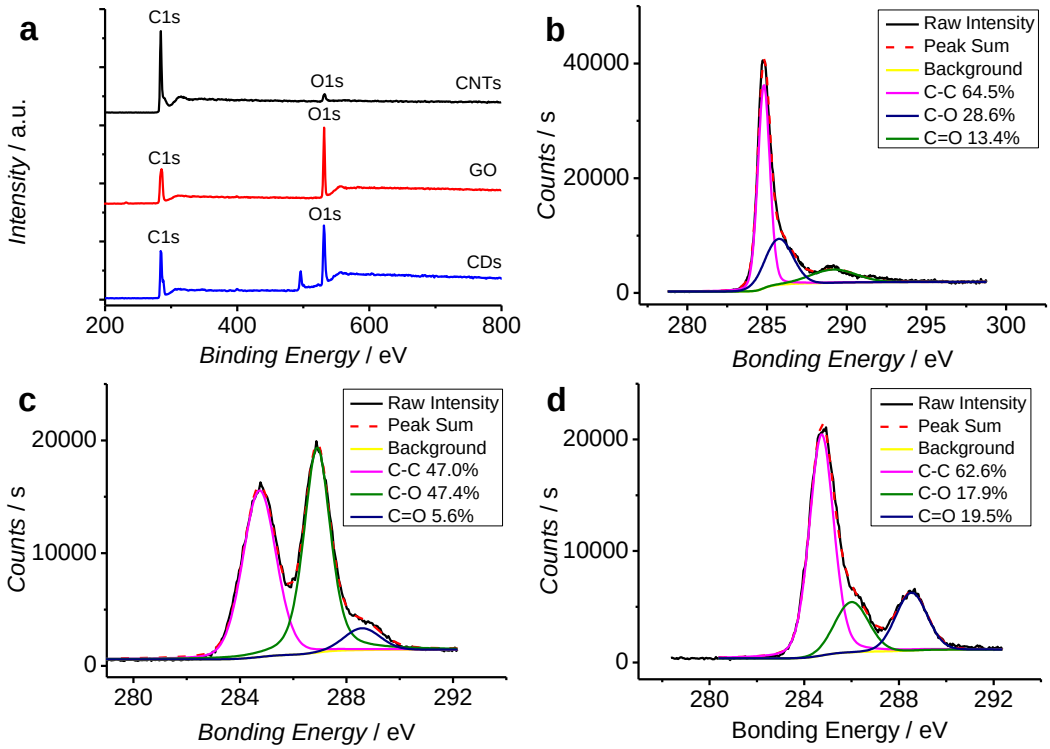

Supplementary Fig. 2. X-ray photoelectron spectroscopy characterization of CNMs. (a) X-ray photoemission spectroscopy profiles of CNTs, GO, and CDs. (b) Curve fit of the C1s peak of CNTs; (c) Curve fit of the C1s peak of GO; (d) Curve fit of C1s peak of CDs. The XPS profiles and C1s core level spectra of the CNMs implied a considerable degree of oxidation. The percentages of sp^2 graphite carbon were 64.5%, 47.0% and 62.6% for CNTs, GO and CDs. The increased components of epoxide group, carbonyl and carboxyl groups facilitated the dispersing of these materials in water.

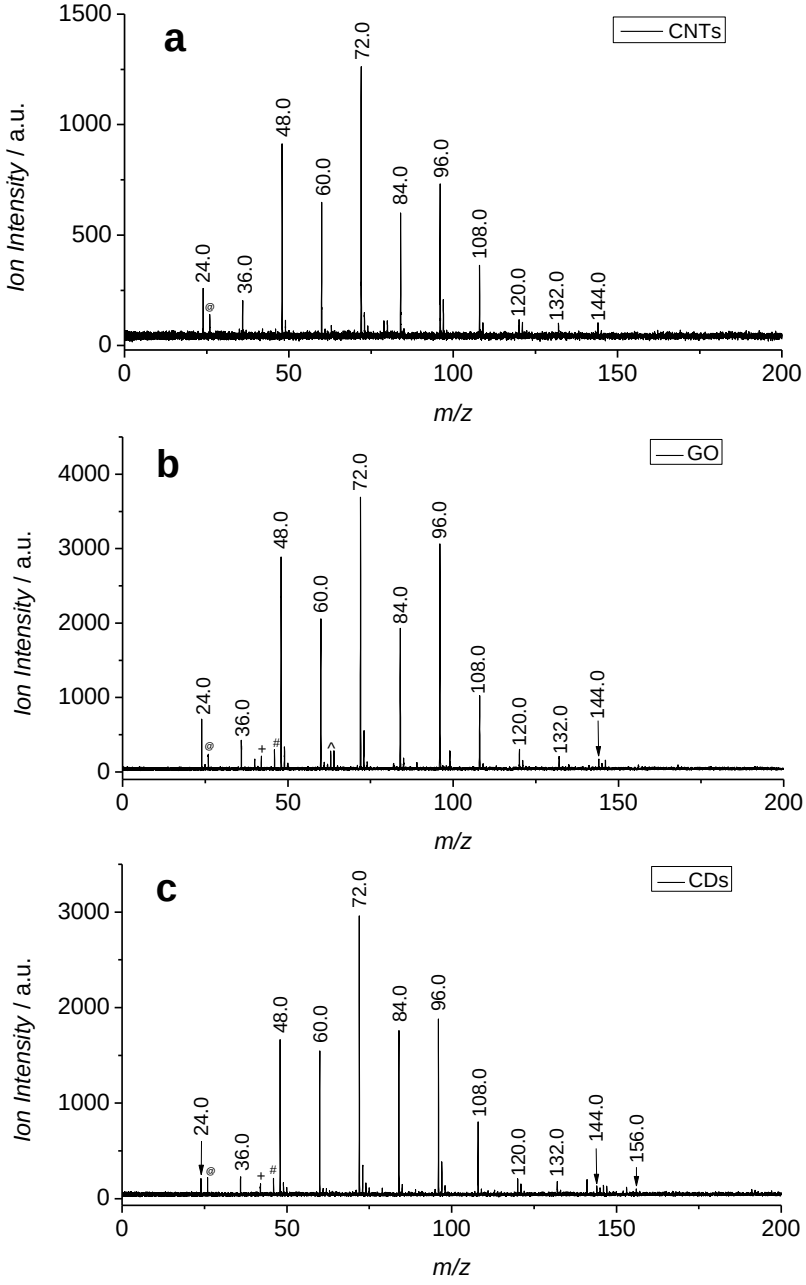

Supplementary Fig. 3. Representative LDI mass spectra of CNMs in negative ion mode. (a) CNTs, (b), GO and (c) CDs. The cluster ions at *m/z* 24.0, 36.0, 48.0, 60.0, 72.0, 84.0, 96.0, 108.0, 120.0, 132.0, 144.0 and 156.0 correspond to the carbon cluster ions C_2^-, C_3^-, C_4^-, C_5^-, C_6^-, C_7^-, C_8^-, C_9^-, C_{10}^-, C_{11}^-, C_{12}^- and C_{13}^-. Other ions in the spectra may correspond to commonly observed photoionization fragments[7] $[CN]^-$ (*m/z* 26.0), $[CNO]^-$ (*m/z* 42.0), $[NO_2]^-$ (*m/z* 46), $[NO_3]^-$ (*m/z* 62.0), which were labeled with (@), (+), (#) and (^), respectively.

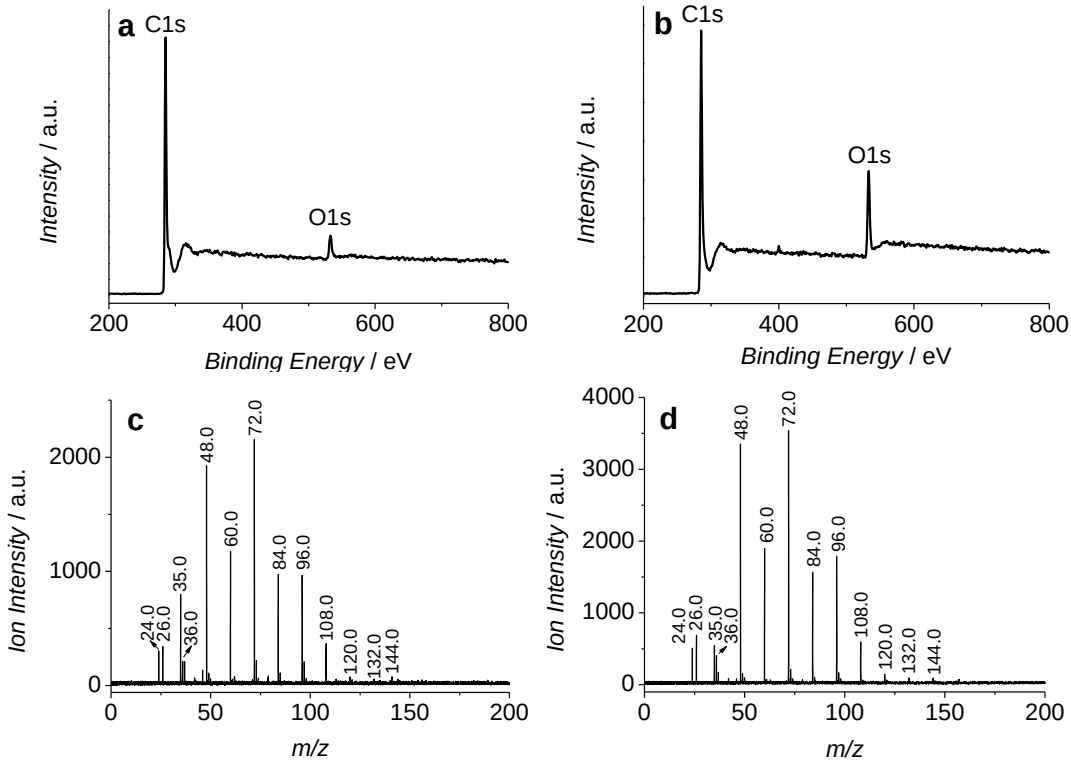

Supplementary Fig. 4. Comparison of CNTs and excessively oxidized CNTs. (a) and (b), X-ray photoemission spectroscopy profiles of CNTs and excessively oxidized CNTs; (c) and (d), representative LDI mass spectra of CNTs and excessively oxidized CNTs. The cluster ions at *m/z* 24.0, 36.0, 48.0, 60.0, 72.0, 84.0, 96.0, 108.0, 120.0, 132.0 and 144.0 correspond to the carbon cluster ions C_2^-, C_3^-, C_4^-, C_5^-, C_6^-, C_7^-, C_8^-, C_9^-, C_{10}^-, C_{11}^- and C_{12}^-. Other ions in the spectra may correspond to commonly observed photoionization fragments $[CN]^-$ (*m/z* 26.0) and $[Cl]^-$ (*m/z* 35.0).

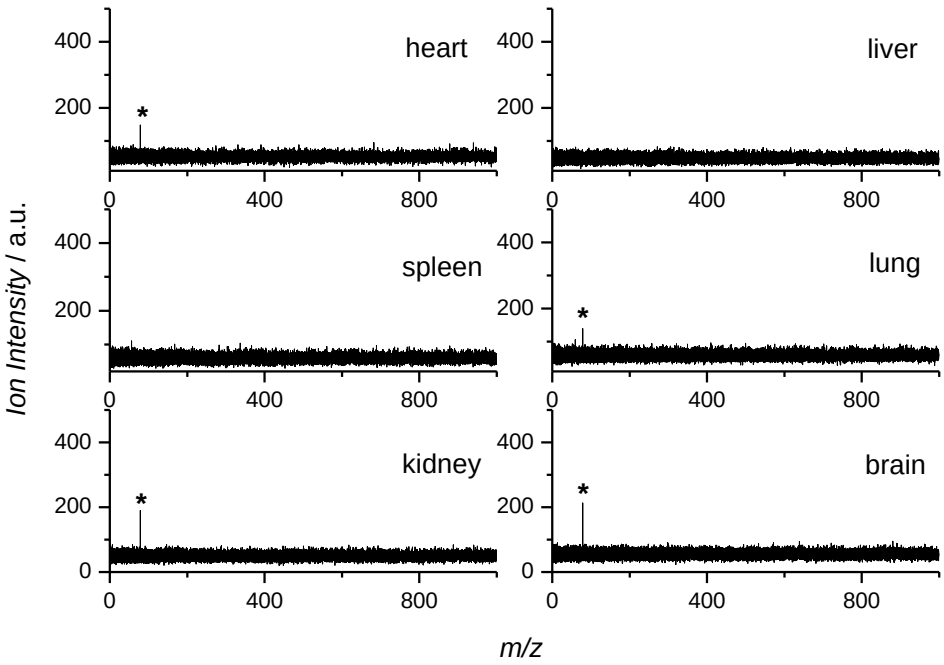

Supplementary Fig. 5. Representative LDI mass spectra of normal mice tissue slice of heart, liver, spleen, lung, kidney and brain in negative ion mode. The ion in the spectra indicated with an asterisk (*) correspond to the common fragment of $[PO_3]^-$ at *m/z* 79.0.[8] The laser energy is 100% for the measurements.

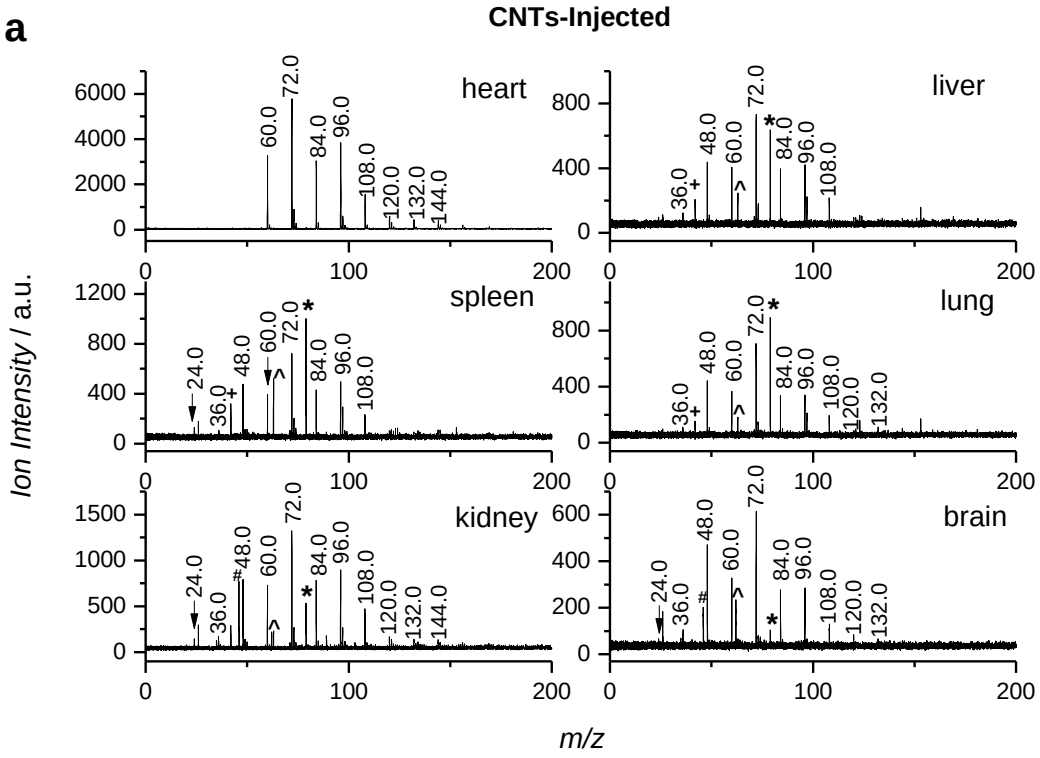

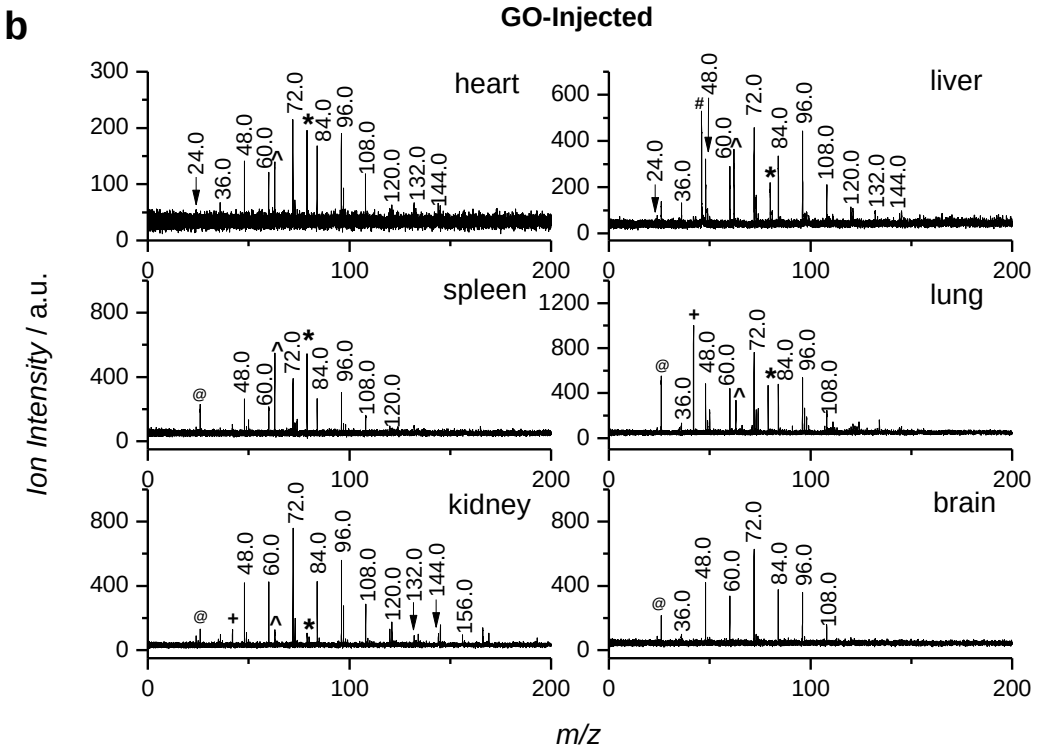

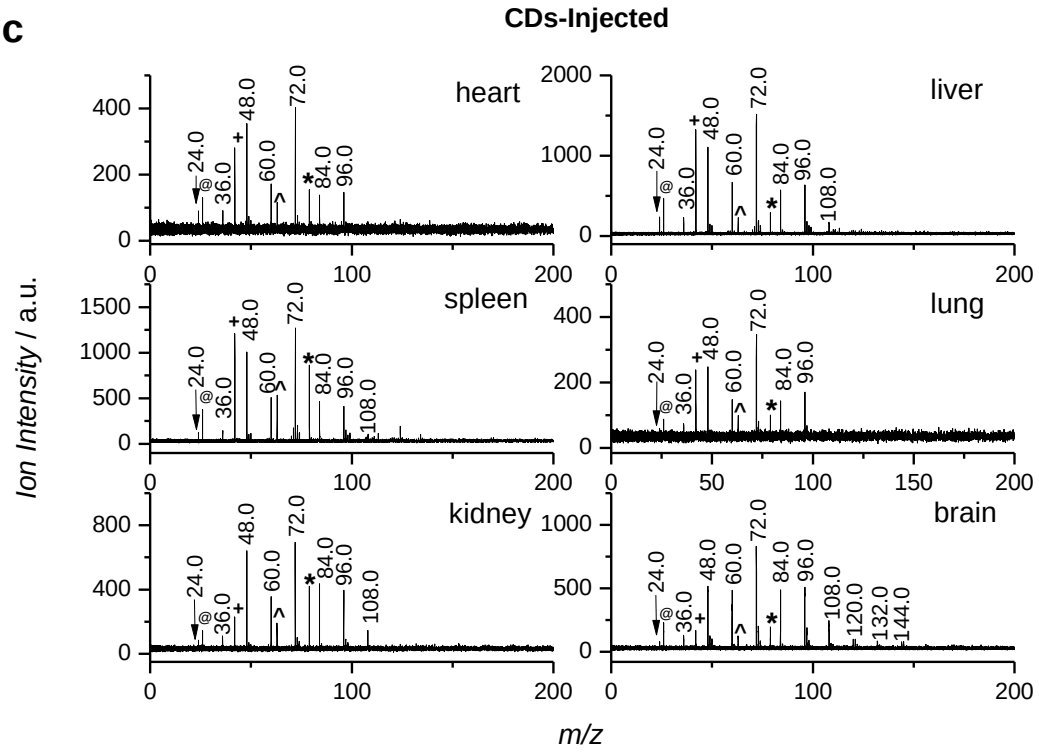

Supplementary Fig. 6. Representative LDI mass spectra of CNMs-injected mice tissue slices of heart, liver, spleen, lung, kidney and brain in negative ion mode. (a) CNT-injected, (b) GO-injected and (c) CDs-injected tissues. The cluster ions at *m/z* 24.0, 36.0, 48.0, 60.0, 72.0, 84.0, 96.0, 108.0, 120.0, 132.0 and 144.0 correspond to the carbon cluster ions C_2^-, C_3^-, C_4^-, C_5^-, C_6^-, C_7^-, C_8^-, C_9^-, C_{10}^-, C_{11}^- and C_{12}^-. Other ions in the spectra correspond to commonly observed photoionization fragments[7] $[CN]^-$ (*m/z* 26.0), $[CNO]^-$ (*m/z* 42.0), $[NO_2]^-$ (*m/z* 46), $[NO_3]^-$ (*m/z* 62.0), $[PO_3]^-$ (*m/z* 79.0), which were labeled with (@), (+), (#), (^) and (*), respectively.

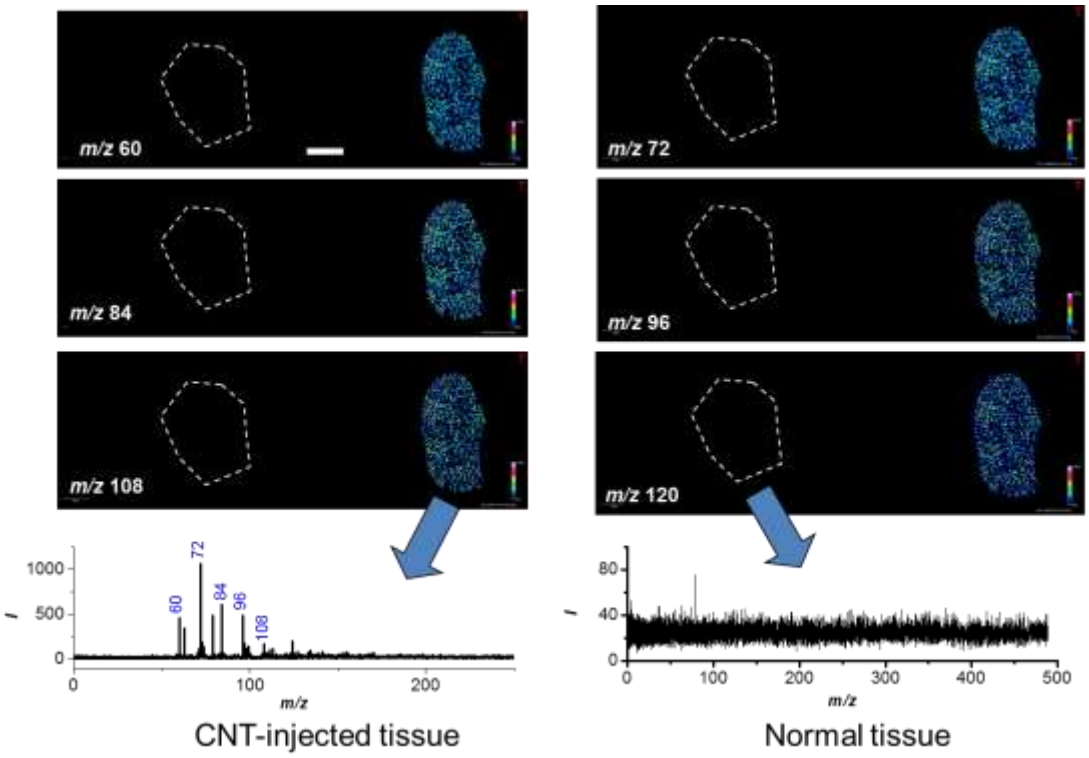

Supplementary Fig. 7. The comparing LDI MS imaging images (upper) and mass spectra (bottom) of normal mouse lung tissue (inside the dash line) and CNTs-injected lung tissue. The mass spectra signals of *m/z* 60, 72, 84, 96, 108 and 120 were chose to generate the imaging images, respectively. The scale bar is 2 mm.

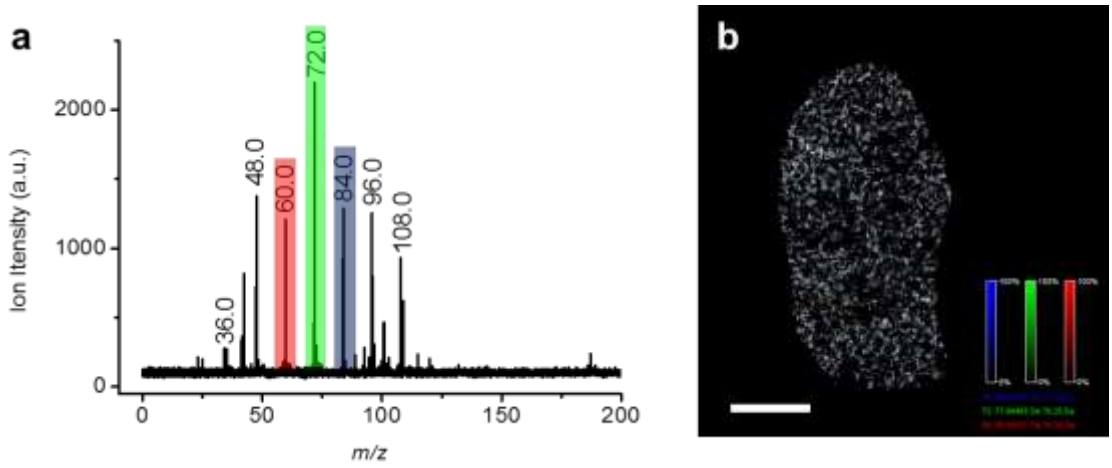

Supplementary Fig. 8. The overlay of different carbon cluster ions images. (a) Representative LDI mass spectrum of CNTs-injected mouse lung tissue and (b) the overlay of the three imaging mass spectrometry images generated by ions at *m/z* 60.0, 72.0 and 84.0. The original image color of each ion is generated by the primary colors red (*m/z* 60.0), green (*m/z* 72.0) and blue (*m/z* 84.0), but the overlay color is white, which indicates all of the ions have equal locations and each of them could represent the distribution of CNTs. The scale bar is 2 mm.

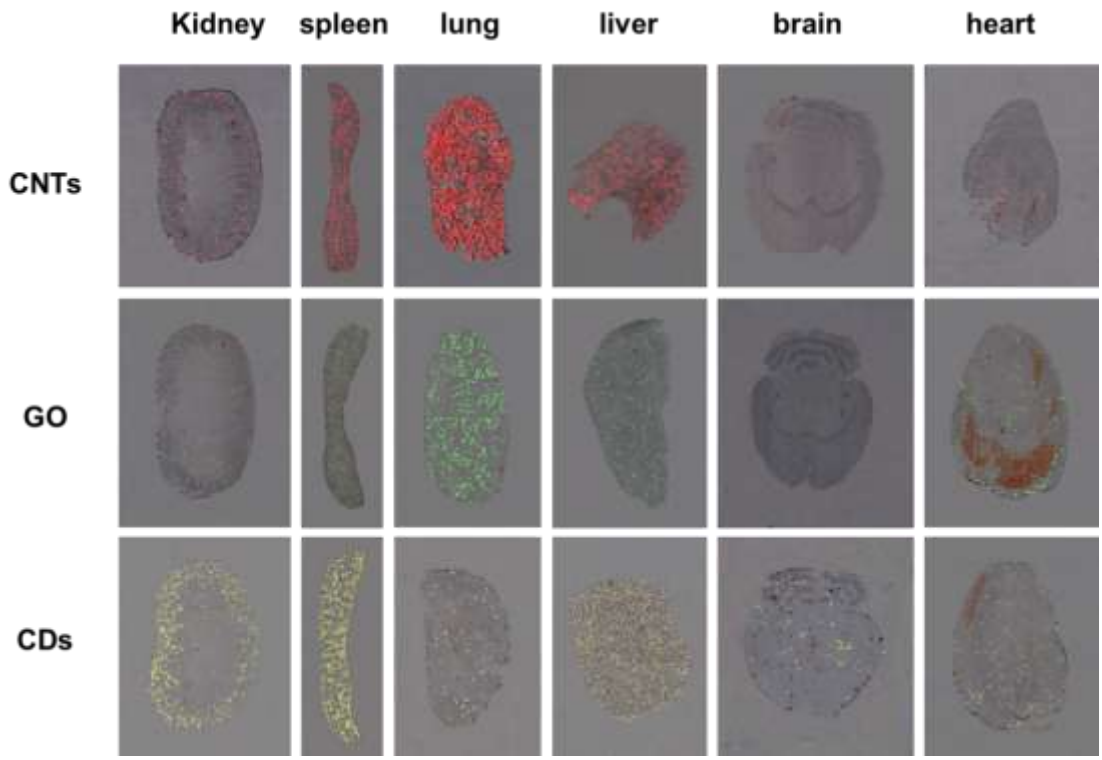

Supplementary Fig. 9. The overlays of LDI mass spectrometry imaging images and optical images of different CNMs-injected tissue slices. C_6^- at *m/z* 72.0 was selected to generate the mass spectrometry imaging images.

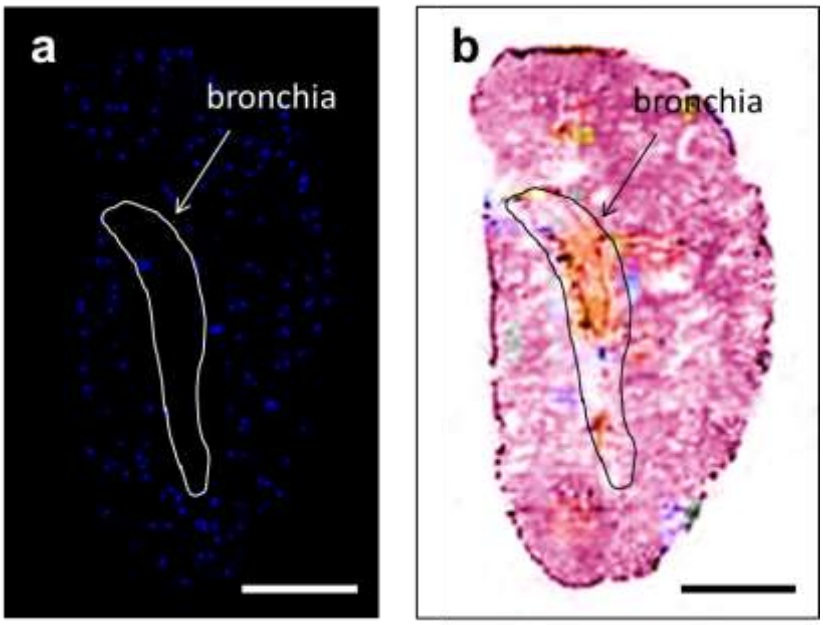

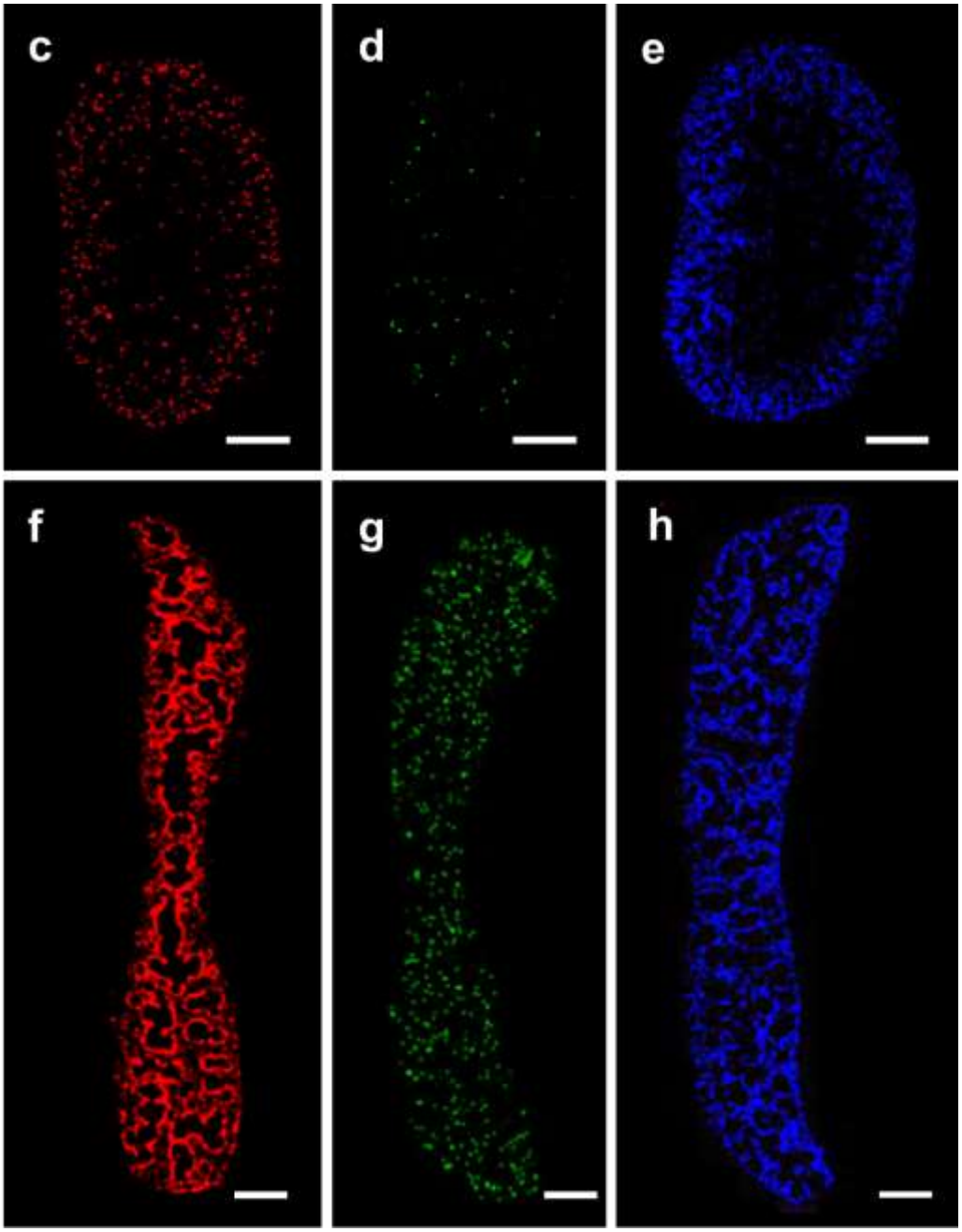

Supplementary Fig. 10. Enlarged LDI IMS images of CNTs, GO and CDs. (a-b) LDI IMS images of CDs-injected mouse lung tissue and its corresponding optical image. (c-e) LDI IMS images of CNTs-, GO- and CDs-injected mice kidney tissues. (f-h) LDI IMS images of CNTs-, GO- and CDs-injected mice spleen tissues. Scale bar: 2 mm.

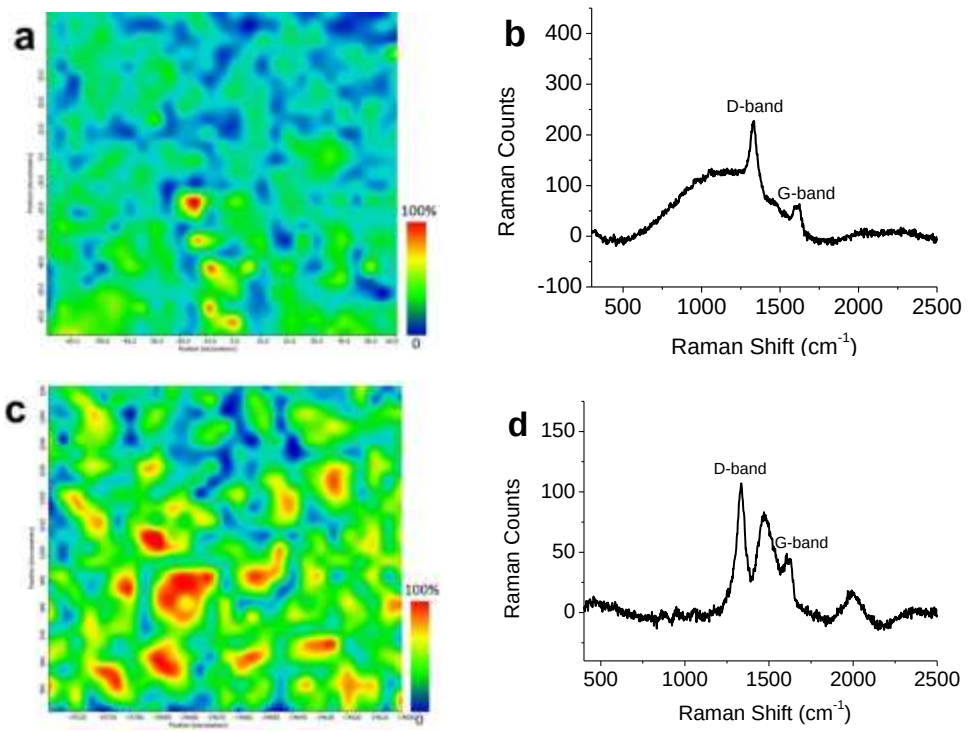

Supplementary Fig. 11. Raman spectroscopy characterization of CNT-injected mouse tissues. (a) Raman mapping image of CNT-injected lung tissue and (b) corresponding Raman spectra. (c) Raman mapping image of CNT-injected liver tissue and (d) corresponding Raman spectra. For Raman mapping, slides were focused in a DXR Raman microscope (Thermo Fisher) and excited with a 780 nm laser (24 mW). The laser spot size is ~ 1 μm. Image was obtained by scanning a 130 μm × 120 μm area in 5 μm × 5 μm steps, and collecting the Raman spectrum at each spot (36 s integration time). G-peak signal at ~ 1600 cm^{-1} was chose to generate the mapping image. The Raman peak between D-band and G-band in (d) may ascribe to the background signal. The red hot spots in mapping image showed the location with high CNTs Raman signals. Three tissue sections from mouse lung and three from liver are examined; and three to five selected regions in each section were scanned by Raman spectroscopy. Although each image is not identical exactly, the patterns of the Raman spectra are similar among the same tissue, which indicate the presence of CNTs.

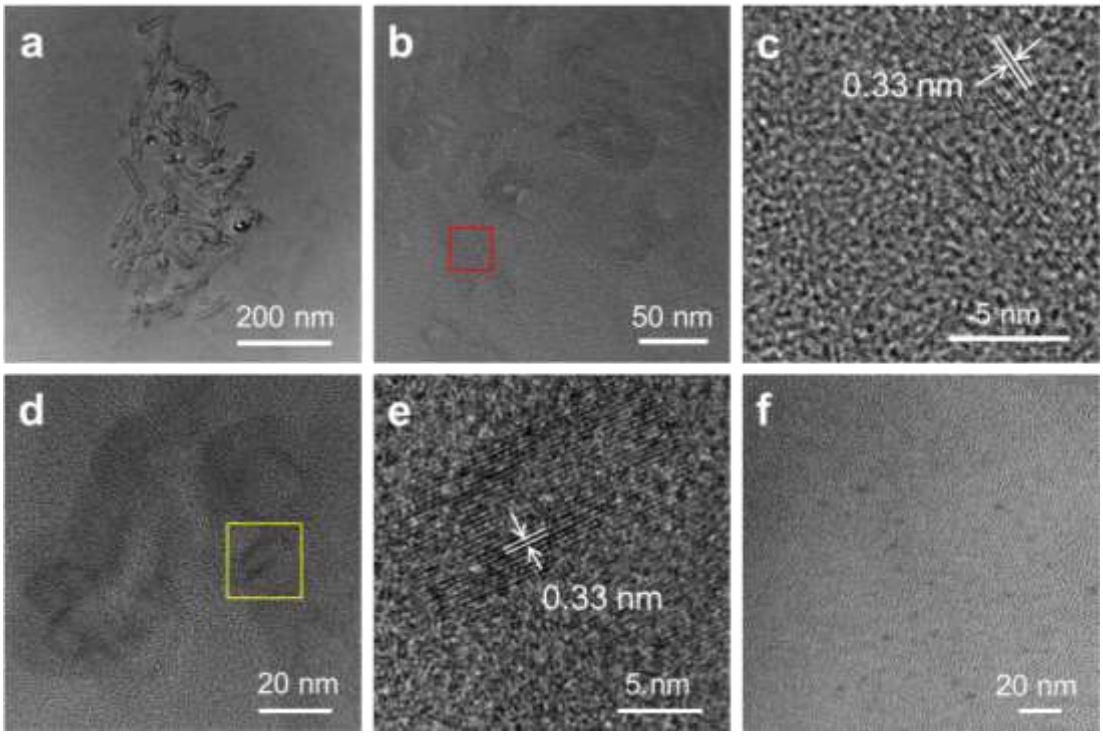

Supplementary Fig. 12. TEM images of CNMs in mice tissues. (a) CNTs in lung tissue. (b) CNTs in spleen tissue. (c) Enlarged HRTEM lattice image of the selected zone (red box) in b. (d) GO in lung tissue. (e) Enlarged HRTEM lattice image of the selected zone (yellow box) in d. (f) CDs in liver tissue. HRTEM measurements revealed lattice spacing of 0.33 nm for CNTs and GO, which is consistent with the (006) diffraction planes of sp^2 graphite carbon (c and e).

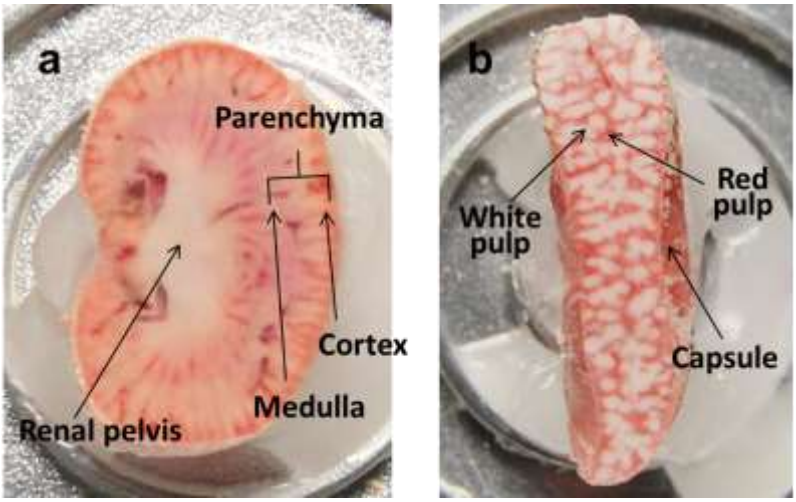

Supplementary Fig. 13. The photographed cross section images of frozen mouse tissue. (a) Kidney, (b) spleen.

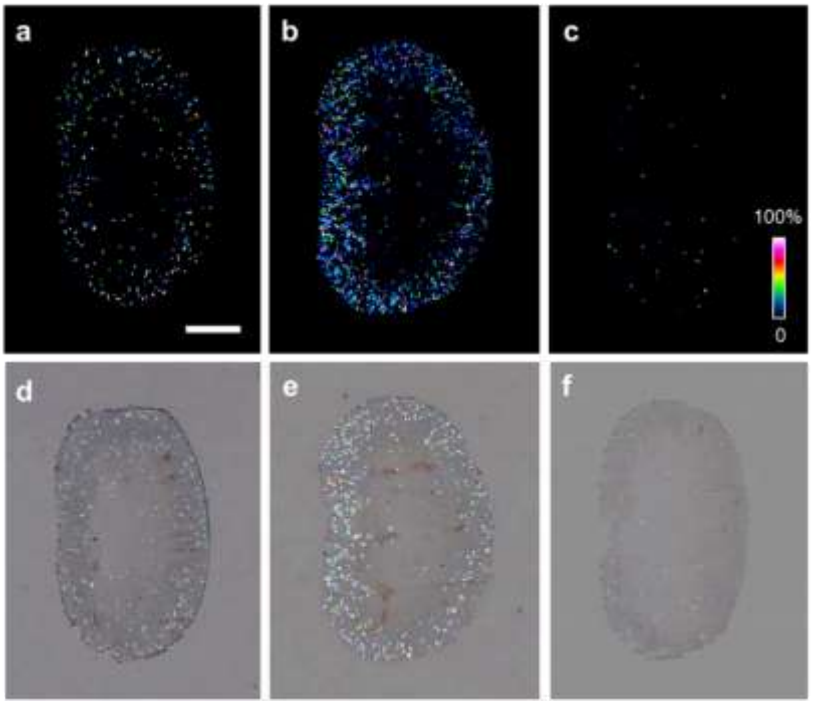

Supplementary Fig. 14. The sub-organ biodistribution of CNMs in mice renal tissues. The top is the heat map for describing the ion intensity distributions (*m/z* 72.0) of (a) CNTs, (b) CDs and (c) GO in renal tissue slices. The bottom is the overlays of the IMS images of (d) CNTs, (e) CDs and (f) GO with respective optical images. The scale bar is 2 mm.

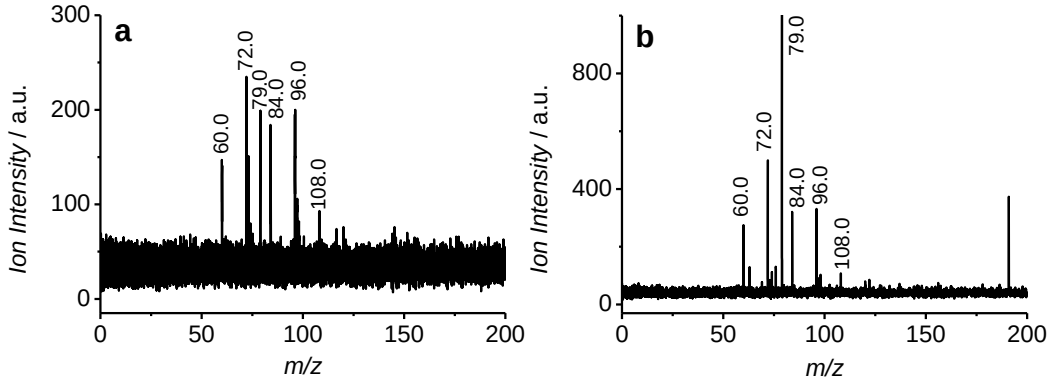

Supplementary Fig. 15. LDI mass spectra of CNMs-injected mice urine. (a) CDs-injected and (b) CNTs-injected mice urine. The cluster ions at *m/z* 60.0, 72.0, 84.0, 96.0 and 108.0 correspond to the carbon cluster ions C_5^-, C_6^-, C_7^-, C_8^- and C_9^-. Ion at *m/z* 79.0 in the spectra correspond to $[PO_3]^-$. The urines were collected from metabolism cages after injection of CDs for 24 h, and diluted for 10 times before direct LDI MS analysis.

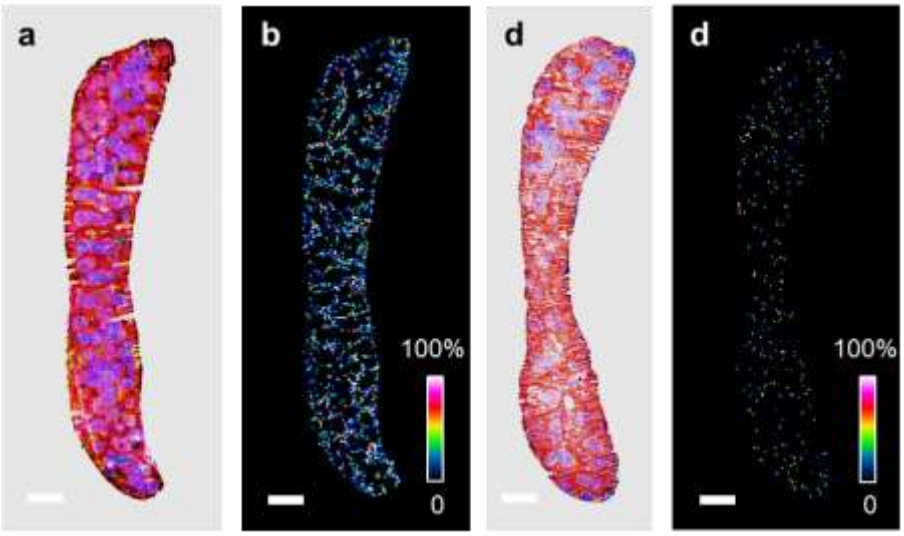

Supplementary Fig. 16. Optical and LDI MSI images of CDs- and GO-injected mouse spleen tissue sections. (a) The optical images of CDs- and (c) GO-injected mouse spleen tissue slices, and their corresponding LDI IMS images (b and d). The ion at *m/z* 72.0 was chose to generate the IMS images, and the scale bar is 2 mm. The color saturation was adjusted to 400% to enhance the contrast.

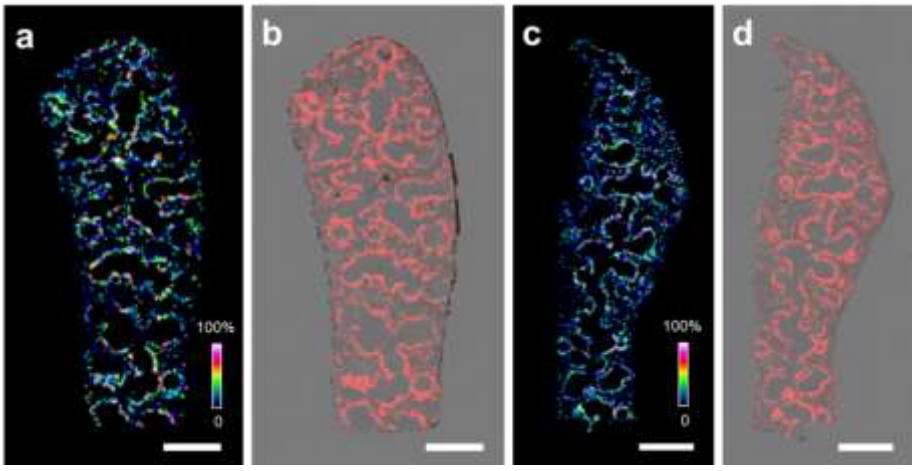

Supplementary Fig. 17. LDI IMS images of CNTs-injected mouse spleen tissue sections. (a) and (c) LDI IMS images of CNTs-injected mice spleen sections and their corresponding (b and d) single color IMS images merged with each optical image. The ion at *m/z* 72.0 was chose to generate the IMS images, and the scale bar is 2 mm.

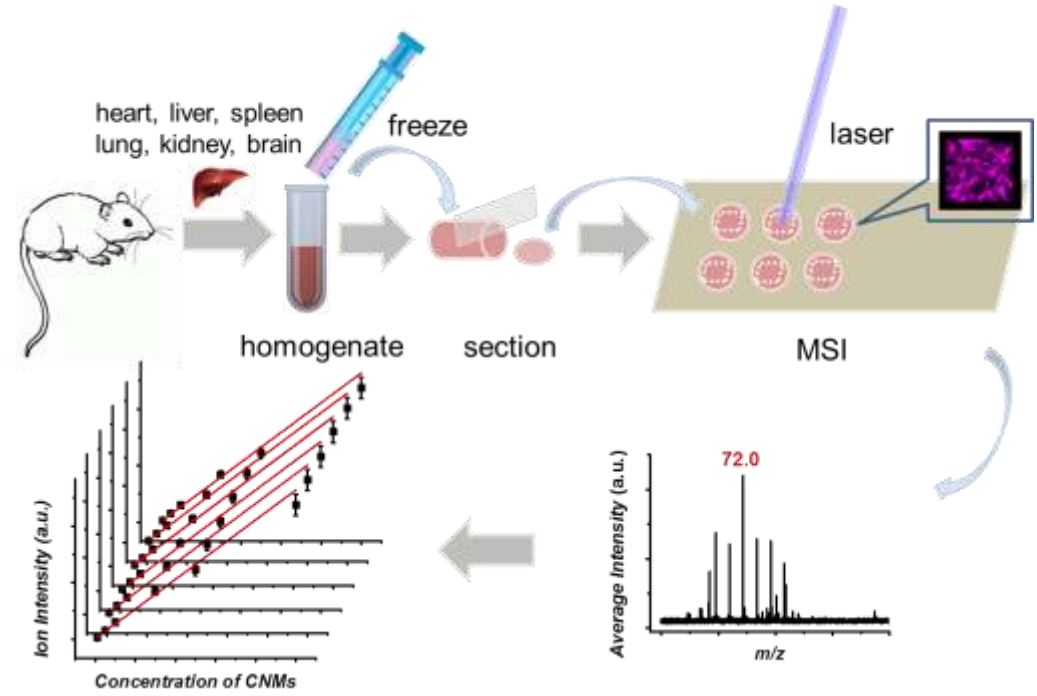

Supplementary Fig. 18. The schematic diagramme of the quantification of CNMs in tissue.

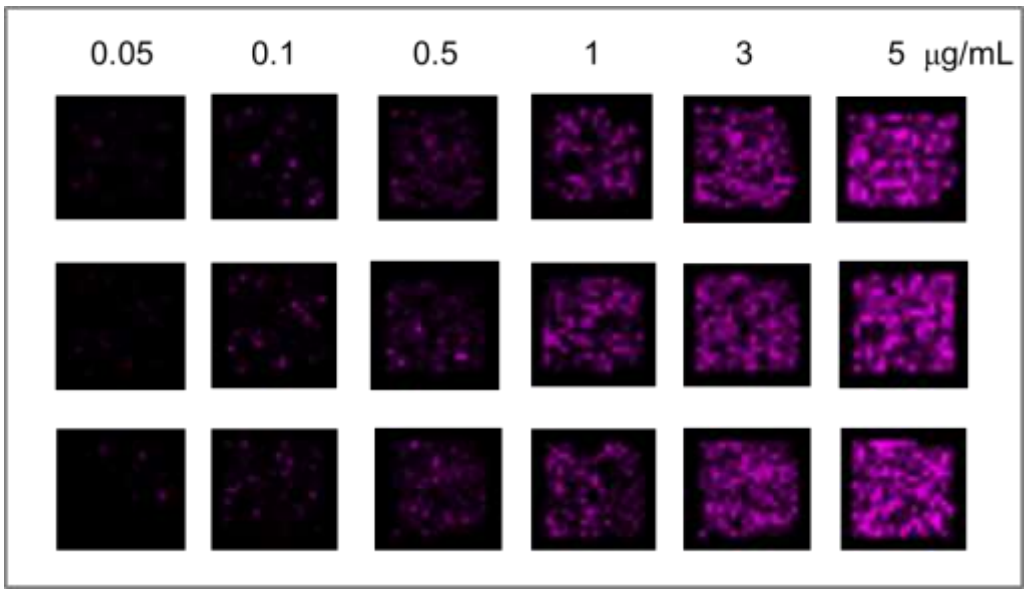

Supplementary Fig. 19. Representative LDI imaging MS images of normal liver homogenate spiked with different concentration of CNTs. Concentrations are 0.05, 0.1, 0.5, 1, 3 and 5 μgmL^{-1}. The three parallel results were showed from the first row to the bottom. The average ion intensity of the imaging area can be read directly from the overall average mass spectrum by using the FlexImaging software.

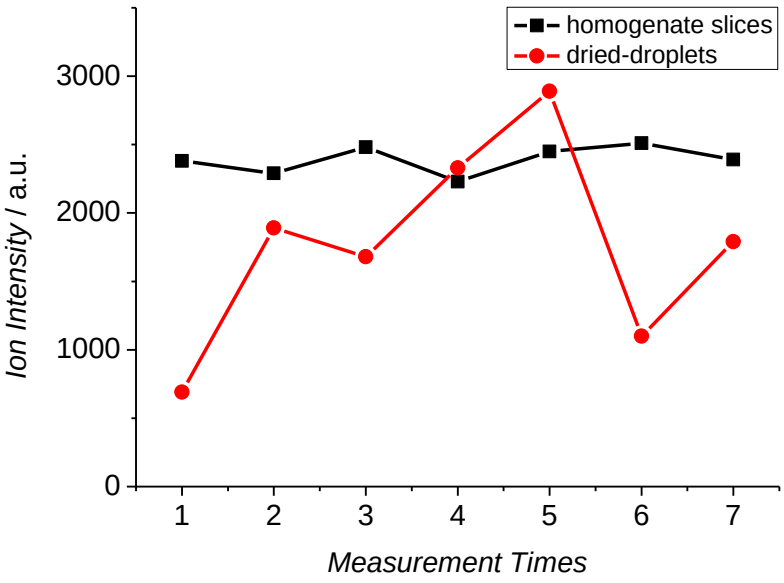

Supplementary Fig. 20. The comparison of the LDI MS reproducibility of homogenate slices and dried-droplets methods under seven times measurements. Mouse Liver homogenate spiked with CNTs was used. The relative standard deviations were 4.2% and 41.4% for the homogenate slices and dried-droplets measurements, respectively.

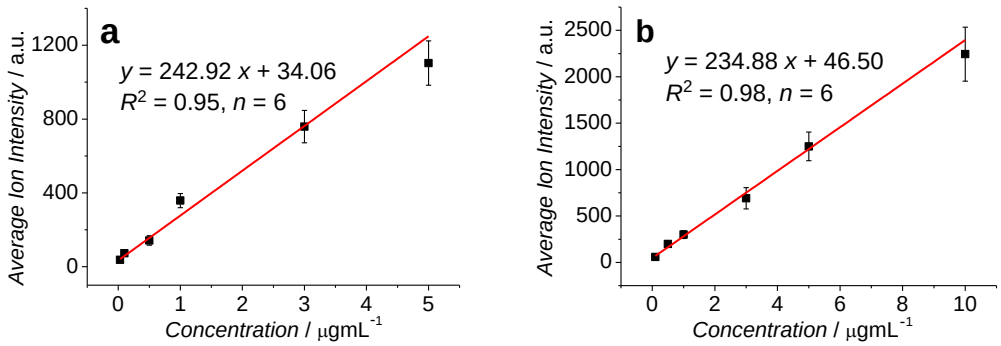

Supplementary Fig. 21. Representative calibration curves for GO and CDs measurements. (a) GO, (b) CDs. These curves were plotted using average ion intensity (*m/z* 72.0) vs. CNMs concentration in liver homogenate. The concentrations are 0.03, 0.1, 0.5, 1, 3, 5 μgmL^{-1} for GO, and 0.1, 0.5, 1, 3, 5, 10 μgmL^{-1} for CDs. All of the linearity ranges are more than two orders of magnitude. Data are presented as the mean ± standard deviation (n = 3).

Supplementary Table 1. The amounts of CNMs in different organs

Material	Organ	% ID/g ± SD	μg/g ± SD	μg ± SD
CNTs	Heart	0.90 ± 0.73	0.90 ± 0.73	0.11 ± 0.08
	Liver	3.29 ± 1.40	3.29 ± 1.40	4.28 ± 1.82
	Spleen	20.90 ± 8.53	20.90 ± 8.53	1.67 ± 0.68
	Lung	55.39 ± 22.02	55.39 ± 22.02	9.97 ± 3.96
	Kidney	4.33 ± 2.22	4.33 ± 2.22	1.73 ± 0.88
	Brain	0.37 ± 0.54	0.37 ± 0.54	0.15 ± 0.22
GO	Heart	0.62 ± 0.24	0.31 ± 0.12	0.05 ± 0.02
	Liver	2.20 ± 1.32	1.10 ± 0.66	1.54 ± 0.93
	Spleen	6.60 ± 3.11	3.30 ± 1.56	0.23 ± 0.11
	Lung	43.22 ± 18.63	21.61 ± 9.31	4.32 ± 1.86
	Kidney	1.12 ± 0.61	0.56 ± 0.31	0.25 ± 0.14
	Brain	0.36 ± 0.54	0.18 ± 0.27	0.08 ± 0.11
CDs	Heart	2.40 ± 0.56	2.40 ± 0.56	0.36 ± 0.08
	Liver	11.81 ± 3.46	11.81 ± 3.46	14.18 ± 4.15
	Spleen	5.50 ± 2.40	5.50 ± 2.40	0.38 ± 0.17
	Lung	2.17 ± 0.86	2.17 ± 0.86	0.35 ± 0.14
	Kidney	3.47 ± 1.03	3.47 ± 1.03	1.73 ± 0.51
	Brain	1.51 ± 0.76	1.51 ± 0.76	0.68 ± 0.34

Supplementary Table 2. Recovery rate tests of the measurements of CNMs in mouse liver homogenate

Sample	Added ($ugmL^{-1}$)	Found ($ugmL^{-1}$)	RSD (%, n = 3)	Recovery rate (%)
CNTs	1.00	0.96	4.86	96.0
	0.50	0.48	3.23	94.0
	0.10	0.11	4.45	110.0
GO	1.00	0.96	5.88	96.0
	0.50	0.52	6.26	104.0
	0.10	0.11	4.90	110.0
CDs	5.00	4.86	4.66	97.2
	1.00	1.06	5.22	106.0
	0.50	0.48	4.64	96.0

Supplementary Table 3. Limits-of-detection of CNMs in different organ homogenates

Organs	Detection of limits (μgmL^{-1})		
	CNTs	GO	CDs
Heart	0.02	0.06	0.10
Liver	0.04	0.03	0.15
Spleen	0.04	0.05	0.20
Lung	0.02	0.05	0.10
Kidney	0.04	0.03	0.20
Brain	0.03	0.03	0.15

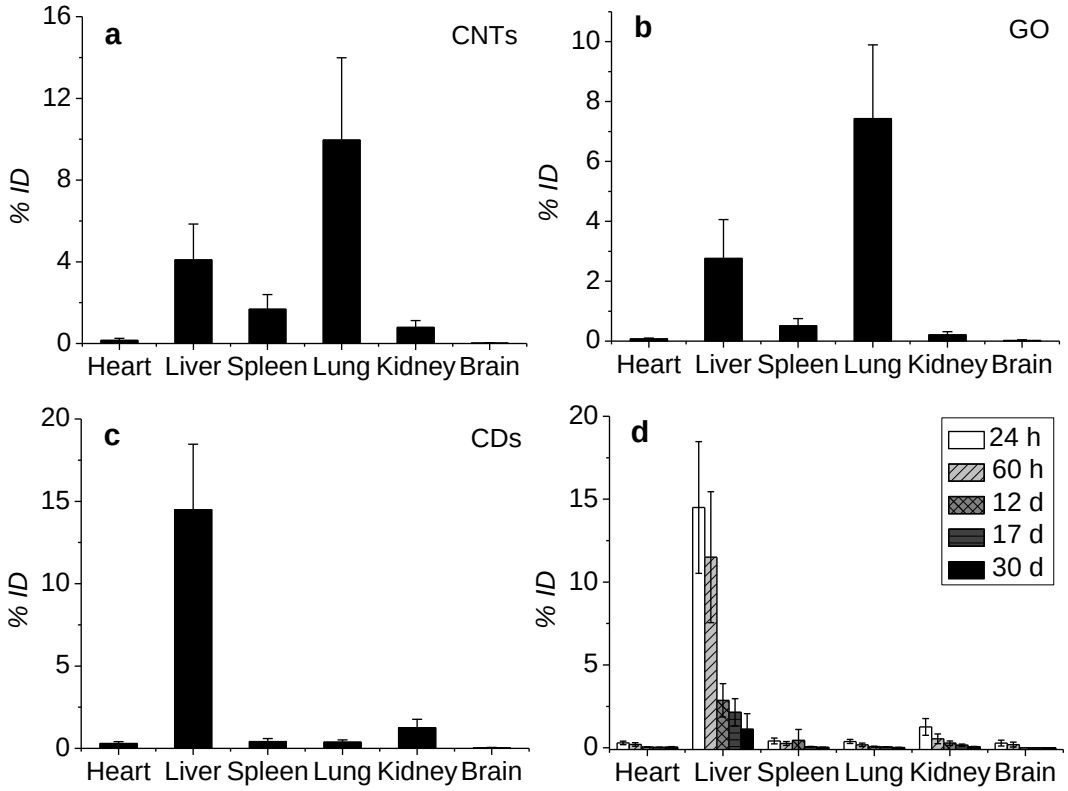

Supplementary Fig. 22. Biodistribution of CNMs in mice. (a) CNTs, (b) GO and (c) CDs at 24 h post-exposure, and (d) biodistribution changes of CDs in different organs measured by LDI MS at 24 h, 60 h, 12 d, 17 d and 30 d post-injection, respectively. Data are presented as the mean ± standard deviation (n = 3), and % ID represents the percentage of the injected dose.

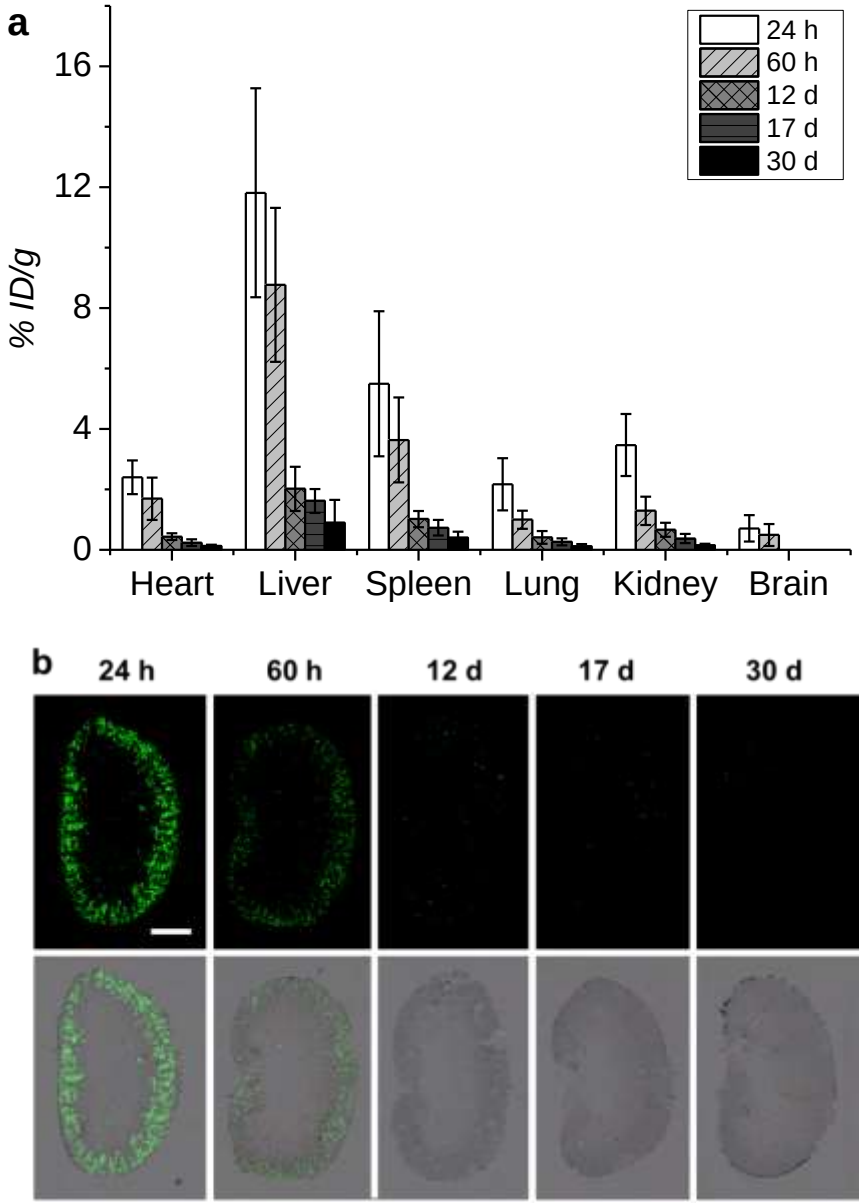

Supplementary Fig. 23. Biodistribution of CDs in mice over time. (a) The biodistribution changes of CDs in different organs measured by LDI MS at 24 h, 60 h, 12 d, 17 d and 30 d p.i., respectively. Data are presented as the mean ± standard deviation (n = 3). (b) The sub-organ distribution of CDs in mice kidney mapped by LDI IMS. The images were generated by C_6^- ion at m/z 72.0, and the scale bar is 2 mm.

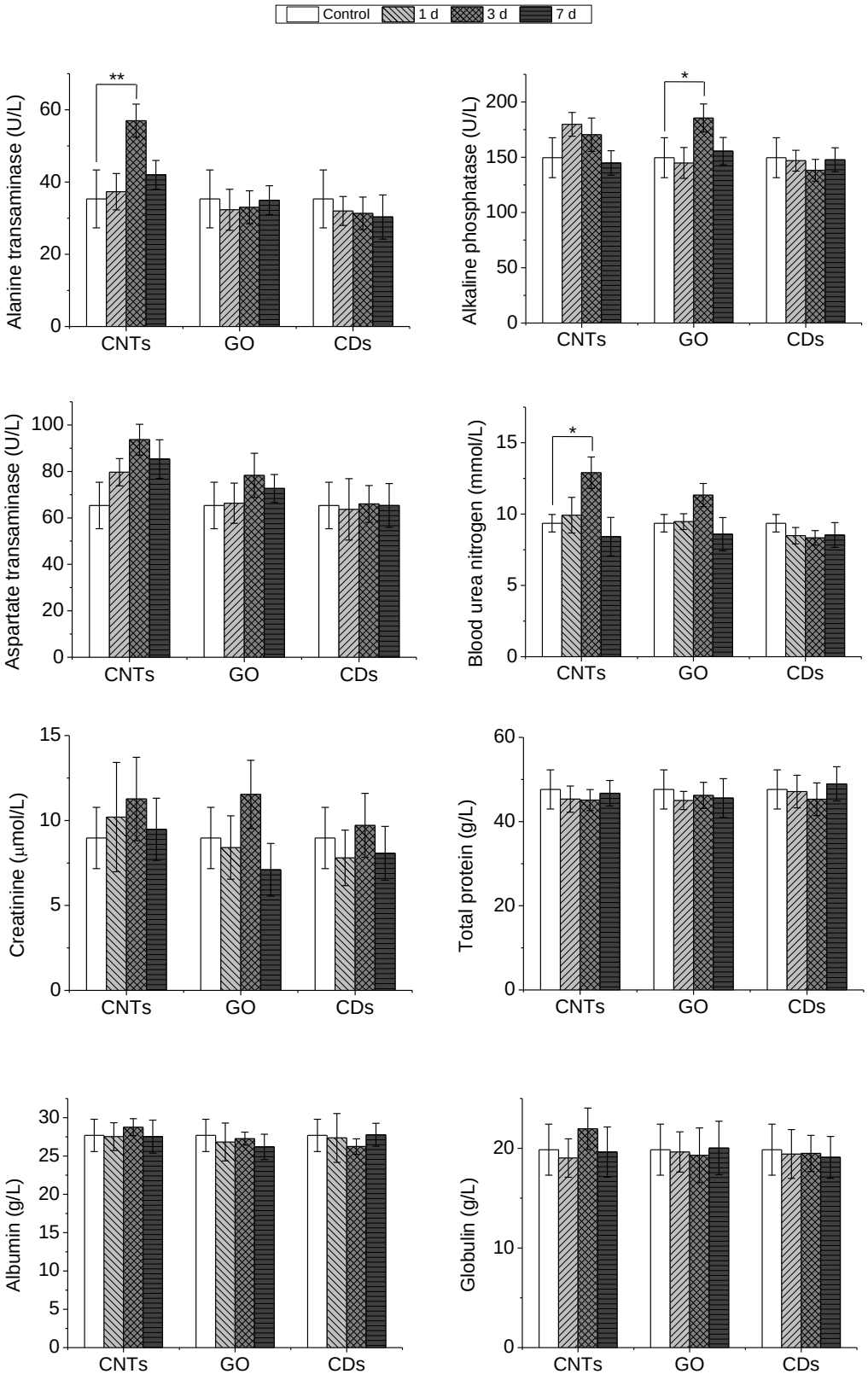

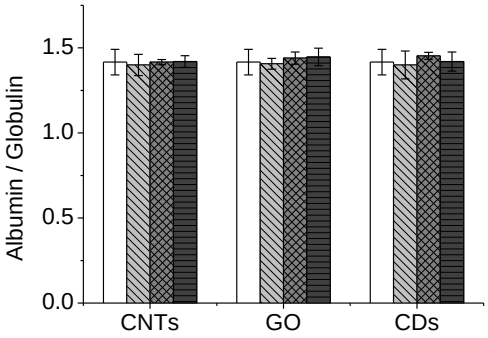

Supplementary Fig. 24. Serum biochemical analysis data of male Kunming mice intravenously administrated with CNTs (4 mgkg^{-1}), GO (2 mgkg^{-1}) or CDs (4 mgkg^{-1}) at 1, 3 and 7 d p.i. Age-matching physiological saline-treated mice were sacrificed at 1, 3 and 7 d p.i. as control. The parameters of the serum biochemical analysis includes: alanine aminotransferase (ALT), alkaline phosphatase (ALP), aspartate aminotransferase (AST), blood urea nitrogen (BUN), creatinine, total protein, albumin, globulin and albumin/globin ratios. Statistics were based on 5 mice per data point.

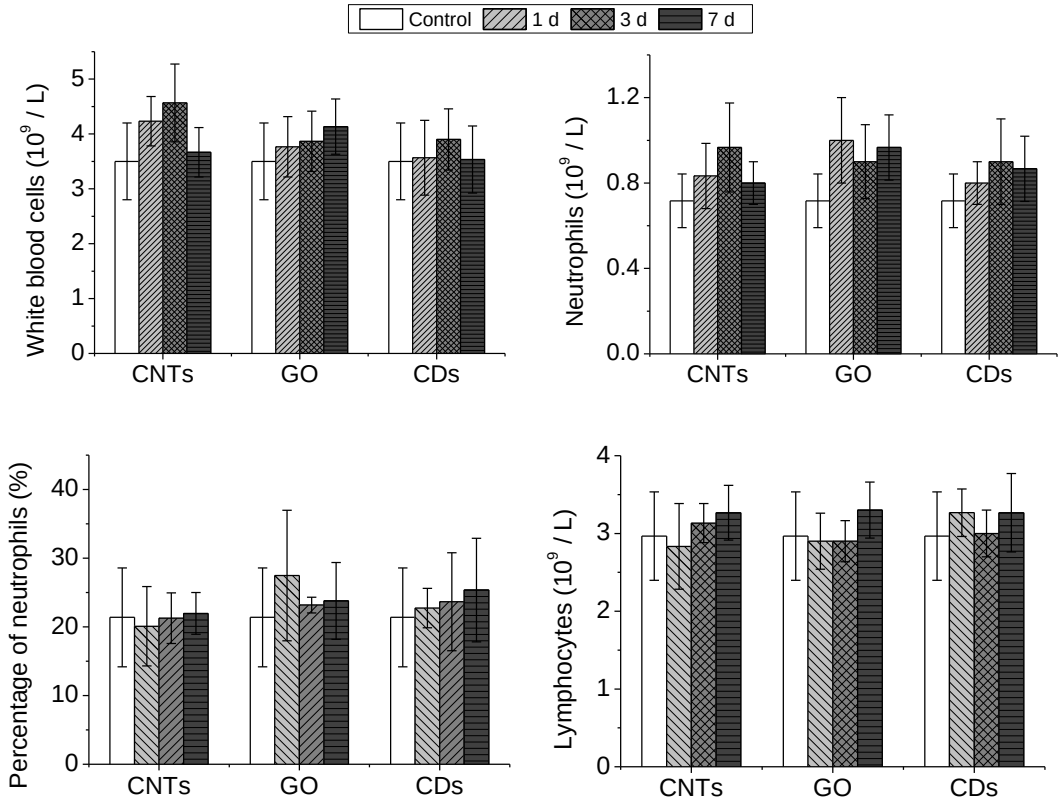

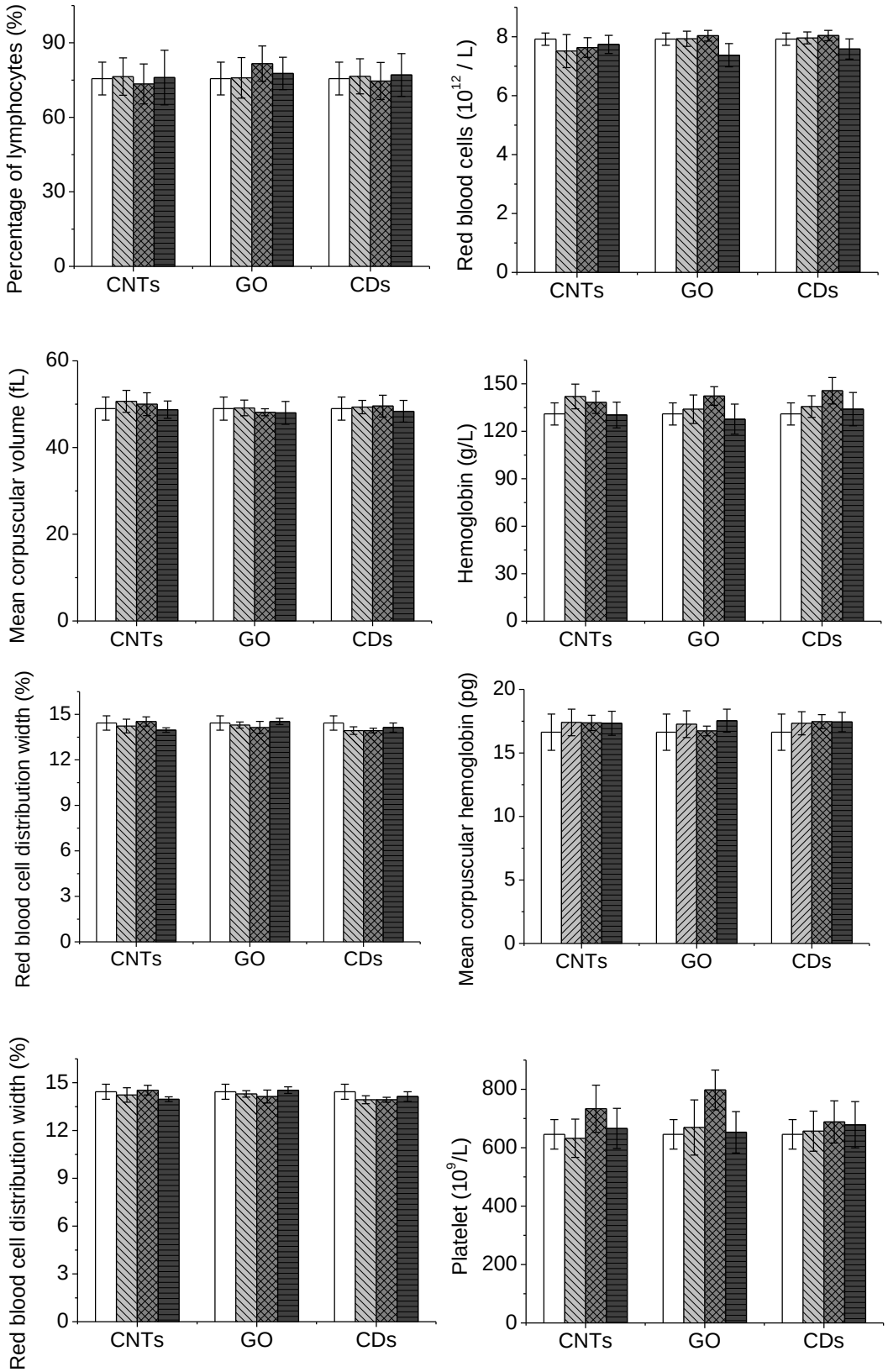

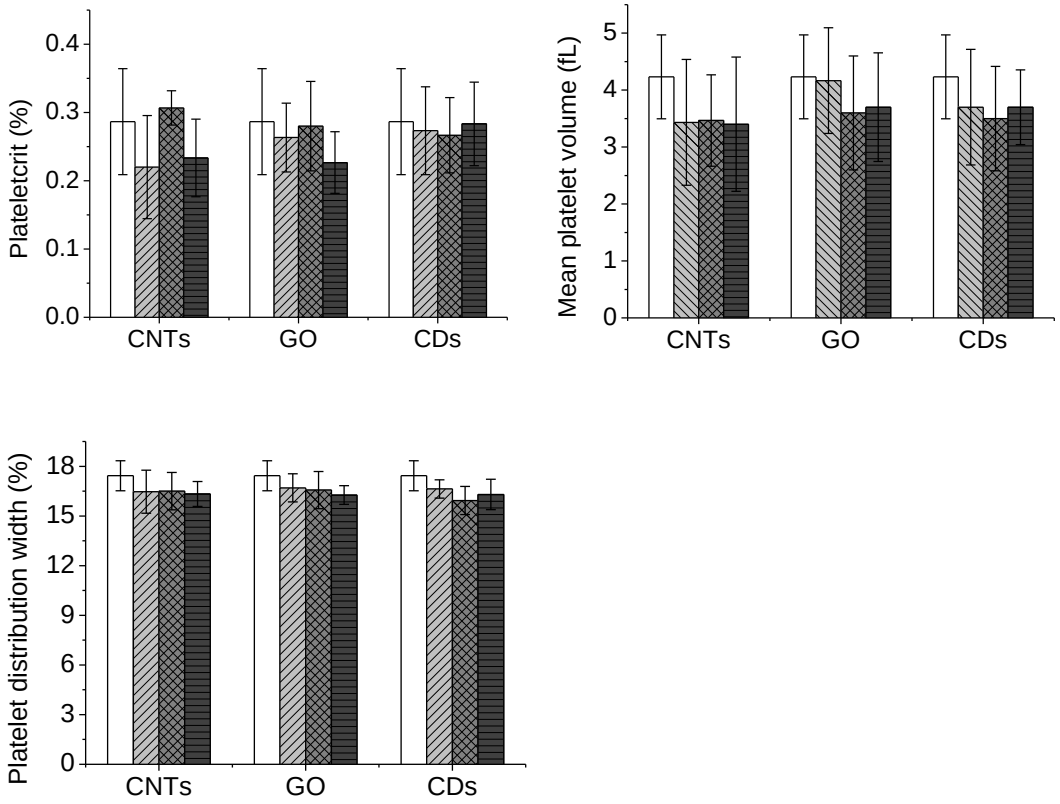

Supplementary Fig. 25. Complete blood counts (CBC) data of male Kunming mice intravenously administrated with CNTs (4 mgkg^{-1}), GO (2 mgkg^{-1}) or CDs (4 mgkg^{-1}) at 1, 3 and 7 d p.i. Age-matching physiological saline-treated mice were sacrificed at 1, 3 and 7 d p.i. as control. The analyzed items for CBC are white blood cells, neutrophils, percentage of neutrophils, lymphocytes, percentage of lymphocytes, red blood cells, mean red cells volume, hematocrit, hemoglobin, mean corpuscular hemoglobin, mean corpuscular hemoglobin concentration, red blood cell distribution width, platelet, mean platelet volume, plateletcrit and platelet distribution width. Statistics were based on 5 mice per data point. No statistically significant difference was found for the CBC data of CNMs-treated mice when compared with saline-treat control mice.

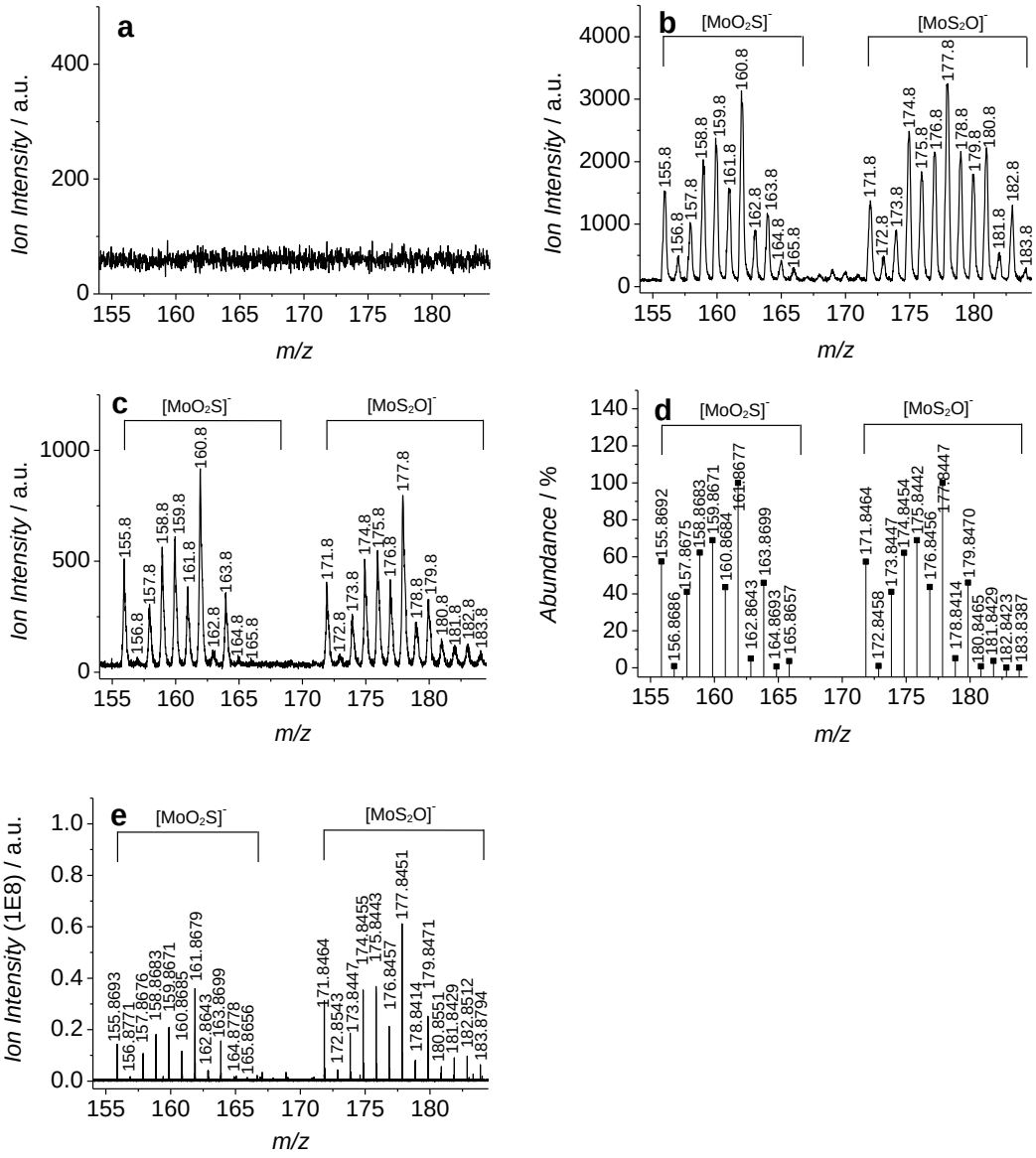

Supplementary Fig. 26. Detection of MoS_2 nanosheets by LDI MS. Typical LDI TOF-MS mass spectra of (a) lung tissue sample from a control mouse, (b) MoS_2 nanosheets from solution, and (c) lung tissue from MoS_2-injected mouse in the negative ion mode. (d) Theoretical isotope patterns of $[MoO_2S]^-$ and $[MoS_2O]^-$. (e) High-resolution MS confirmation of $[MoO_2S]^-$ and $[MoS_2O]^-$ by Fourier transform ion cyclotron resonance mass spectrometry (FT-ICR MS, solariX, Bruker Daltonics) equipped with Nd:YAG/355 nm laser. External calibration was carried out in quadratic mode using sodium trifluoroacetate to obtain five points of calibration over the mass range.

References

[1] S. Chen, H. Zheng, J. Wang, J. Hou, Q. He, H. Liu, C. Xiong, X. Kong, Z. Nie, *Anal. Chem.* **2013**, *85*, 6646-6652.

[2] S. L. Koeniger, N. Talaty, Y. Luo, D. Ready, M. Voorbach, T. Seifert, S. Cepa, J. A. Fagerland, J. Bouska, W. Buck, R. W. Johnson, S. Spanton, *Rapid Commun. Mass Spectrom.* **2011**, *25*, 503-510.

[3] M. Lagarrigue, R. Lavigne, E. Tabet, V. Genet, J. P. Thome, K. Rondel, B. Guevel, L. Multigner, M. Samson, C. Pineau, *Anal. Chem.* **2014**, *86*, 5775-5783.

[4] X. L. Huang, F. Zhang, L. Zhu, K. Y. Choi, N. Guo, J. X. Guo, K. Tackett, P. Anilkumar, G. Liu, Q. M. Quan, H. S. Choi, G. Niu, Y. P. Sun, S. Lee, X. Y. Chen, *ACS Nano* **2013**, *7*, 5684-5693.

[5] H. Tao, K. Yang, Z. Ma, J. Wan, Y. Zhang, Z. Kang, Z. Liu, *Small* **2011**, *8*, 281-290.

[6] a) Z. Liu, X. Sun, N. Nakayama-Ratchford, H. Dai, *Acs Nano* **2007**, *1*, 50-56; b) Z. Liu, A. C. Fan, K. Rakhra, S. Sherlock, A. Goodwin, X. Chen, Q. Yang, D. W. Felsher, H. Dai, *Angew. Chem. Int. Ed.* **2009**, *48*, 7668-7672.

[7] T. J. Kauppila, T. Kotiaho, R. Kostiainen, A. P. Bruins, *J. Am. Soc. Mass Spectrom.* **2004**, *15*, 203-211.

[8] M. Edelson-Averbukh, R. Pipkorn, W. D. Lehmann, *Anal. Chem.* **2006**, *78*, 1249-1256.